

## CHAPTER 3

### RESULTS AND DISCUSSIONS

This results from platinum-based ternary catalysts were divided into three groups which were PtCoCr, PtCoM (M=Cu,Cr,Fe and Ni) and PtCuNi groups.

The first group provided the results of PtCoCr as a catalysts supported on treated and untreated carbon (Vulcan XC-72) by microwave and NaBH<sub>4</sub> reduction methods. The catalysts were selected by the overview study which that platinum-based ternary catalyst in the form of PtCoCr/C was the highest performance among ternary catalysts [31,46,70,71]. This research focused on the catalysts formation between two methods, particle size, size distribution and particle dispersion on treated and untreated carbon supporters.

In the second group, PtCoM type (M=Cu,Cr,Fe and Ni) was synthesized as a catalyst supported on treated carbon N115 by reflux method. This group of catalyst used the PtCo catalyst as a base catalyst because the overview binary catalysts found that the PtCo was the highest performance [37,72,73]. The PtCo catalyst was added one metal to form ternary catalysts. The metals were added in this catalyst such as copper, chromium, iron and nickel.

For the final group, PtCuNi type was synthesized as a catalyst supported on treated carbons by microwave, reflux, and NaBH<sub>4</sub> reduction method. The research focused on this catalyst because the standard reduction potentials of platinum and copper were positive ( $E^\circ_{\text{Pt}}=1.18$ ,  $E^\circ_{\text{Cu}}=0.37$ ). However, standard reduction potentials of nickel was - 0.257, so it was difficult to be reduced to metal. In order to prove that nickel ion could be reduced to nickel metal, the experiment was performed by

dissolving nickel nitrate in ethylene glycol. The  $\text{NaBH}_4$  was added for a reduction process and the reaction was allowed to stir overnight. The final product was filtered, washed with methanol and dried in oven for overnight. The product was annealed at  $600\text{ }^\circ\text{C}$  for 4 hours under  $\text{N}_2$  gas. The XRD patterns showed in Figure 3.1 indicate that no signal of nickel phase was observed from the pristine sample. However, the signal of nickel was found from the annealed sample at  $2\theta = 44.52, 51.92$  and  $76.40$  with corresponding to (111), (200) and (220) plane of Ni (JCPDS No. 00-004-0850). The results confirm that nickel ion was able to be reduced to nickel metal by  $\text{NaBH}_4$ . The absence of nickel signal primitive sample might be because of amorphous nickel phase containing in the sample [74-75]. From the evidence, PtCuNi catalyst was feasibly synthesized in this study.

The results were explained in two parts. In the first part, the result of treated carbon was explained. Whereas, the results of catalysts on supported carbon prepared by technique was explained in the second part.

### **3.1 Treated and untreated carbons analyses**

The functional group modification on carbon surface was applied to two types of carbon which were carbon Vulcan XC-72 and carbon N115. The physical properties of both carbons were shown in Table 3.1 and shapes of both carbons were shown in Figure 3.2 by TEM technique. The shape and particle size of both carbons were similar. The particle size from carbon Vulcan XC-72 and carbon N115 were  $32.85 \pm 5.54$  and  $32.99 \pm 7.94$  nm, respectively. The particle size histograms from carbon were shown in Figure 3.3. For other reason, carbon N115 was made in Thailand (Thai Carbon Black Public Co. LTD).

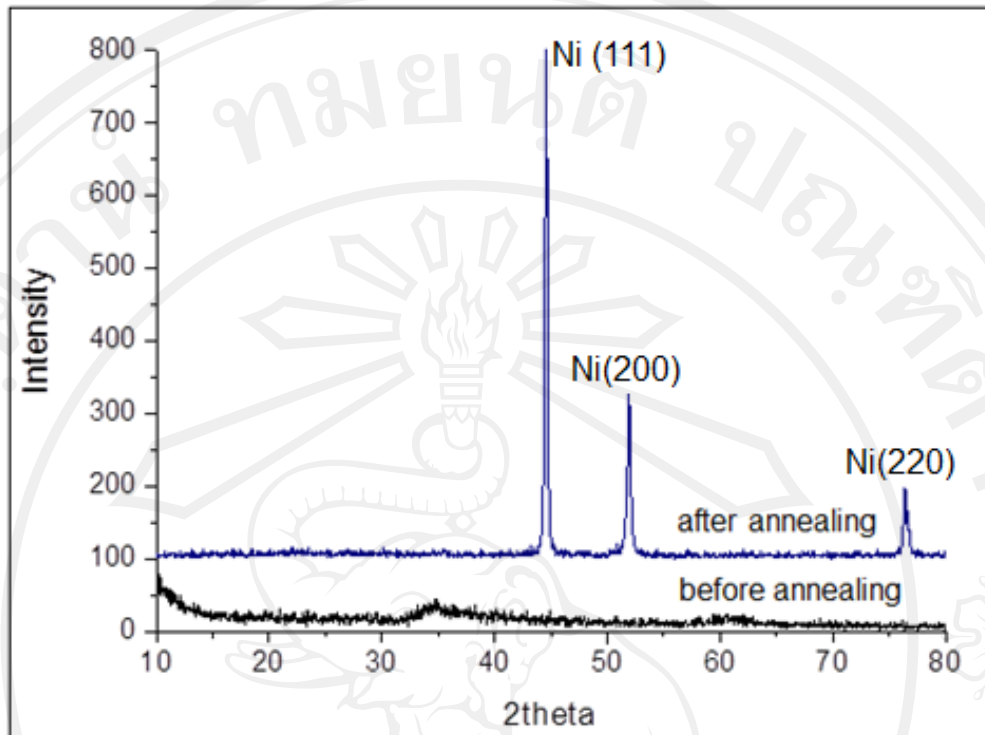


Figure 3.1 Powder XRD patterns of nickel prepared by  $\text{NaBH}_4$  reduction method for before (below) and after (upper) annealing samples.

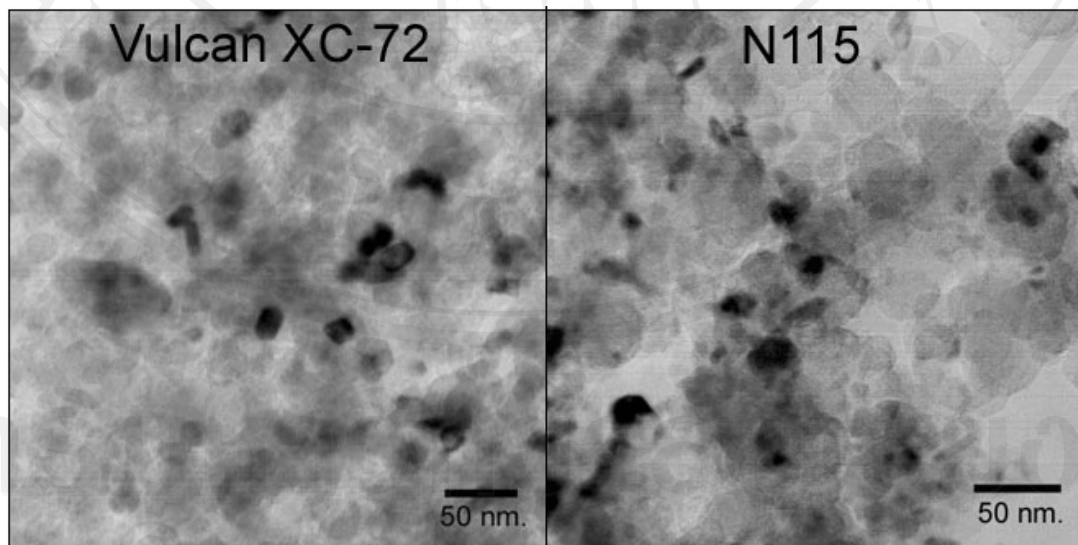


Figure 3.2 TEM images of carbon Vulcan XC-72 and carbon N115

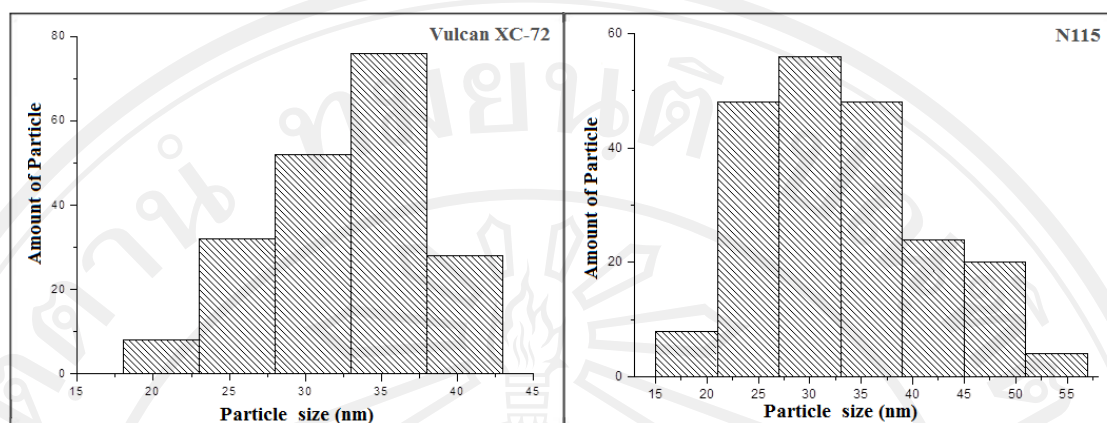


Figure 3.3 Particle size histograms of carbon Vulcan XC-72 and carbon N115

Table 3.1 The physical properties of carbon Vulcan XC-72 and carbon N115

Carbon	Vulcan XC-72	N115
Specific surface area ( $\text{m}^2/\text{g}$ )	254[76]	146.4[77]
Conductivity (s/cm)	4.0[76]	$7.99 \times 10^{-7}$ [78]
Particle size (nm)	$32.85 \pm 5.54$	$32.99 \pm 7.94$
DBP ( $\text{cm}^3/100 \text{ g}$ )	175[79]	94.0[77]
Pour density ( $\text{kg}/\text{m}^3$ )	264[80]	345[81]
Porous area ( $\text{m}^2/\text{g}$ )	76[80]	137[81]

In comparison, both treated and untreated carbons were characterized by FTIR technique as shown in Figure 3.4. It can be seen that the untreated carbon's bands at  $2357$ ,  $2015$  and  $1591 \text{ cm}^{-1}$  were corresponded to the vibration of  $-\text{C}\equiv\text{C}-$ ,  $-\text{C}=\text{C}=\text{C}-$  and  $-\text{C}=\text{C}-$ , respectively. Whereas, the carbon treated by hydrogen peroxide were detected the bands at  $2362$ ,  $2038$  and  $1647 \text{ cm}^{-1}$  and were corresponded to the vibration of  $-\text{C}\equiv\text{C}-$ ,  $-\text{C}=\text{C}=\text{C}-$  and  $-\text{C}=\text{C}-$ , respectively, which were similar to the untreated carbon. However, a small band at  $1693 \text{ cm}^{-1}$  and  $1518 \text{ cm}^{-1}$  were additionally detected

which was identified as  $\text{-C=O}$  of carboxylic group and  $(\text{-C(=O)-O-})$ , respectively. The appearance of this functional group was due to hydrogen peroxide which acted as a strong oxidizing agent[82] and can oxidize the carbon-carbon bond on carbon surface to carboxylic group[83,84]. The mechanism for this reaction was shown in Eq 3.1. The carboxylic group, with a negatively charged functional group in solution is shown in Eq 3.2. This functional group can improve the formation of Pt-based ternary catalysts on carbon due to electrostatic interaction between metal ion, which is a positive charge, and carboxylic group (negative charge).

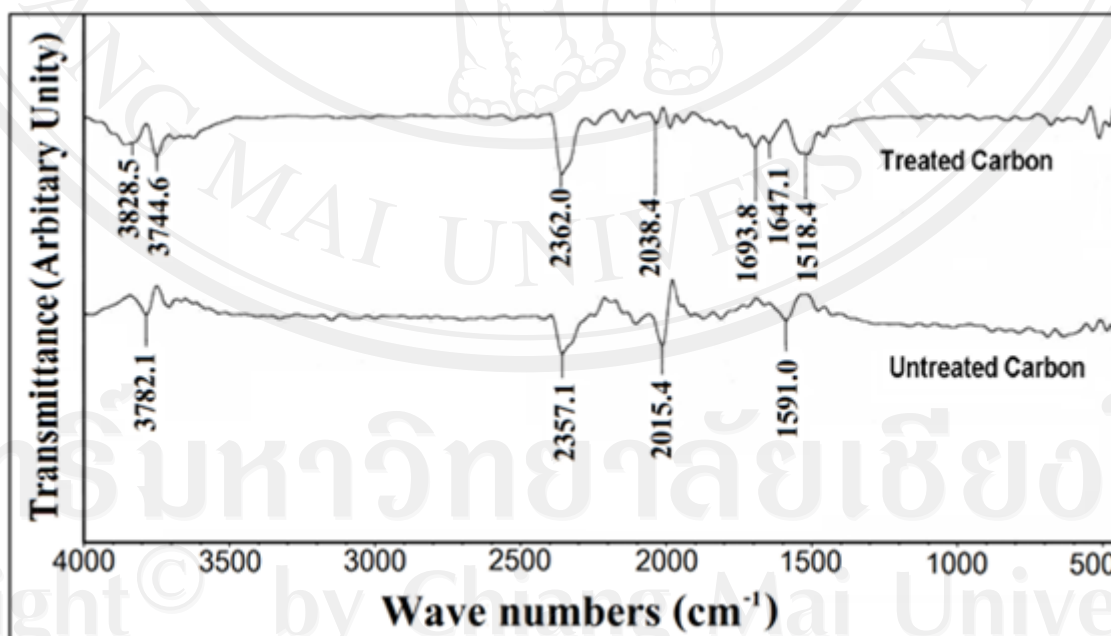
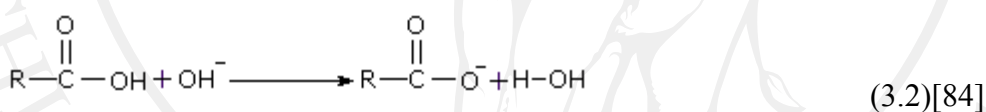
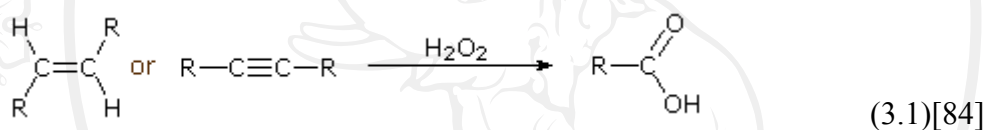


Figure 3.4 FTIR spectrums from treated carbon and untreated carbon

### 3.2 The Characterization

The catalysts were firstly characterized the physical properties by XRD, SEM, EDS, TEM and XAS technique. Second, the electrochemical properties were investigated by CV and single cell testing. XRD technique was used to identify the sample phases. SEM technique was used to observe metals dispersion on carbon supporter. Elemental composition and quantity was analyzed by EDS technique. While particle size and size distributions of metals were observed by TEM technique. The XAS technique was used to indicate the oxidation number and local structure of metals. CV technique was included in this study in order to test the electro-catalytic activity of prepared sample. Moreover, single cell testing provides plot of polarization curve which was performed to investigate cell performance.

#### 3.2.1 Powder X-ray diffraction (XRD)

All catalysts were characterized by XRD technique. In Figure 3.5 – 3.8, broad peak at  $2\theta \approx 25.34^\circ$  was observed corresponded to (002) plane of carbon (JCPDS No. 00-041-1487). For the catalysts in the first group, metal phases containing in catalysts from microwave and  $\text{NaBH}_4$  reduction method were compared (Figure 3.5). For the catalysts from microwave method, only platinum peak at  $2\theta = 39.80$  was found which corresponded to (111) plane of platinum (JCPDS No. 00-004-0802). While other diffracted planes of platinum was not obviously observed because there was a small amount of platinum containing in the sample (it was which confirmed by EDS). The absence of other diffracted planes of platinum was assured by the intensities on plane (200) and (220) as 53 and 31 which was lower than baseline. The metals such as cobalt, chromium or metal oxide were also not clearly observed as they appeared in

the area of platinum broad peak or their small amount in samples. The catalysts from  $\text{NaBH}_4$  reduction method were unclearly observed in those XRD patterns. Peak broadening was possibly influenced small particle size where the unclear metals peaks might be because of small particles size effect and small amount of metals. Therefore, the SAD and XAS were then applied to identify the occurrence of these metals.

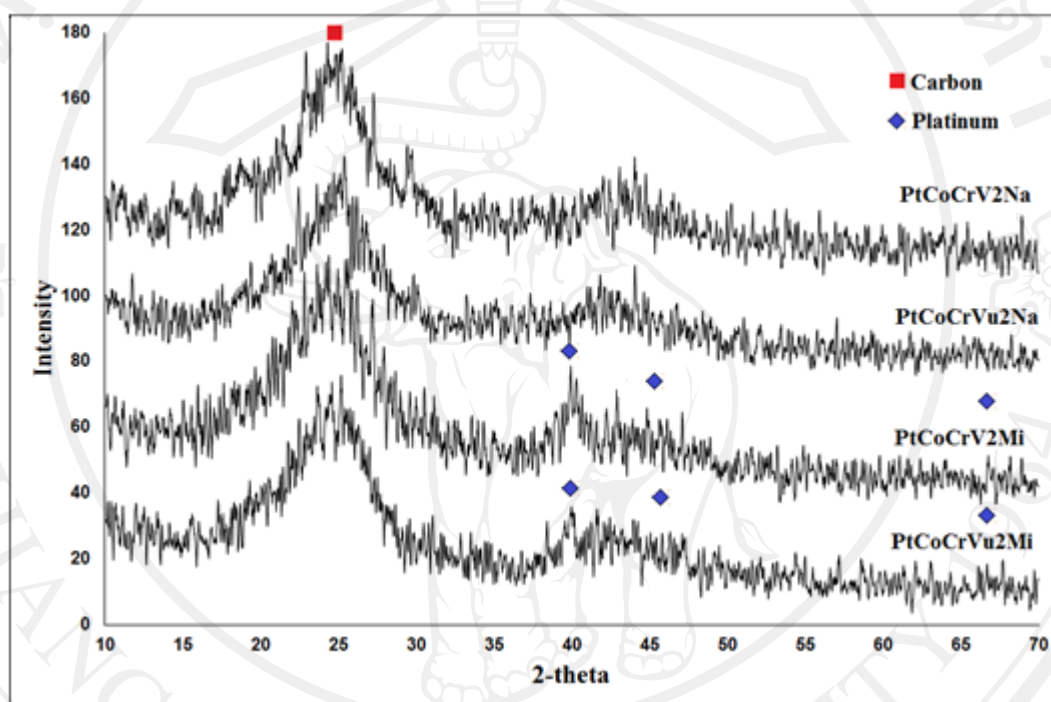


Figure 3.5 Powder XRD patterns of platinum-cobalt-chromium catalysts supported on treated or untreated carbon by microwave and  $\text{NaBH}_4$  reduction methods

The XRD patterns of second group catalysts shown in Figure 3.6. In this group, other transition metals (Cu, Cr, Ni, and Fe) was changed when the binary catalyst was fixed as PtCo alloy. The result for this group was separated into two parts. First part was PtCoCu catalyst and second part was other catalysts. The PtCoCu catalyst in the first part showed the diffracted peak at  $2\theta = 40.93, 47.23$  and  $69.37$  which corresponded to (111), (200) and (220) planes of PtCoCu alloy (Simulated unit cell by

CaRIne V3.1 from Patent No. 5,178,971 was shown in Figure 3.9). For other catalysts in the second part, (PtCoNi, PtCoFe and PtCoCr) showed the peaks at  $2\theta = 39.63$ ,  $46.29$  and  $67.25$  which corresponded to (111), (200) and (220) planes of platinum. However, the other metal (Co, Cr, Ni, and Fe) or metal oxides were unclearly observed because of the smallest particle size or lowest amount of metals support on carbon. Therefore, the electron diffraction was further used to identify them.

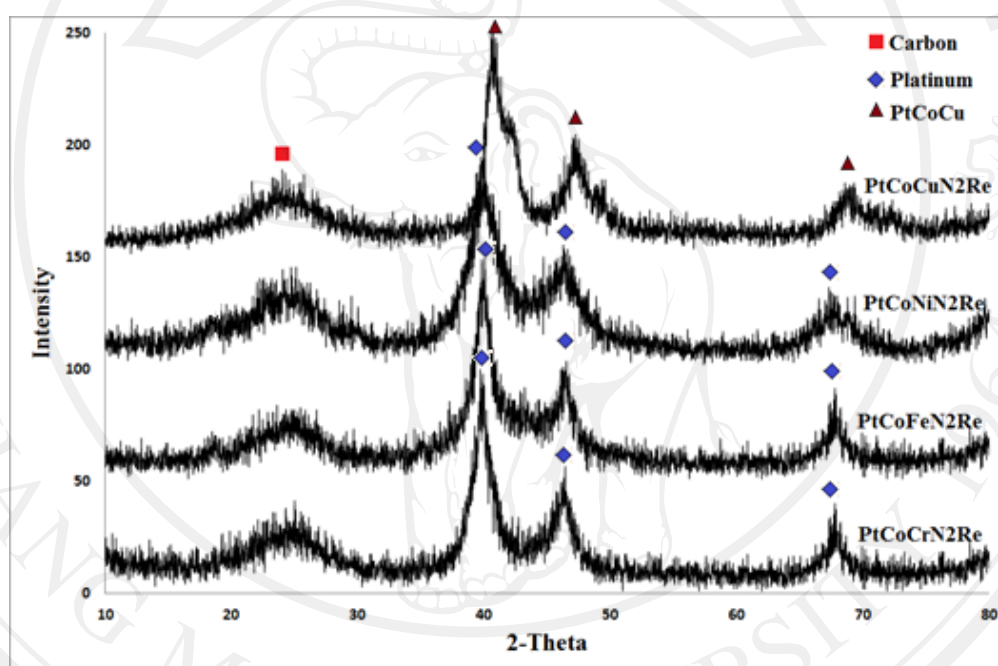


Figure 3.6 Powder XRD patterns of platinum-cobalt-metal catalysts supported on treated carbon by reflux method.

The XRD patterns of third group catalyst were shown in Figure 3.7-3.8. The catalysts in this group were prepared by three methods (microwave, reflux, and  $\text{NaBH}_4$  reduction method) on two types of carbon (VulcanXC-72 and N115) with two weight ratio (2:1:1 and 6:1:1). The catalysts supported on carbon N115 with the ratio 2:1:1 and ratio 6:1:1 were shown in Figure 3.7. In contrast, the catalysts supported on

carbon Vulcan XC-72 with the ratio of 2:1:1 and 6:1:1 were shown in Figure 3.8. The results of all catalysts in this group were separated into two parts. First part, the catalysts were prepared by microwave method and in the next part, the catalysts were prepared by reflux and  $\text{NaBH}_4$  reduction methods. Catalysts which synthesized by microwave at ratio of 2:1:1 and 6:1:1 showed peak at  $2\theta = 39.80, 46.16$  and  $67.44$  with corresponding to (111), (200) and (220) plane of platinum. The XRD patterns from this part showed only platinum peak while the other metals (Cu and Ni) or metal oxide were unclearly observed because of the small amount of metals supported on carbon. Next part, catalysts showed broad peaks at  $2\theta = 41.12, 47.85$  and  $69.99$  with corresponded to (111), (200) and (220) plane of PtCuNi alloy (Simulated unit cell by CaRIne V3.1 from Patent No.5,178,971 was shown in Figure 3.10). The XRD patterns for all samples showed broad peaks for metal alloy because small particle size effect.

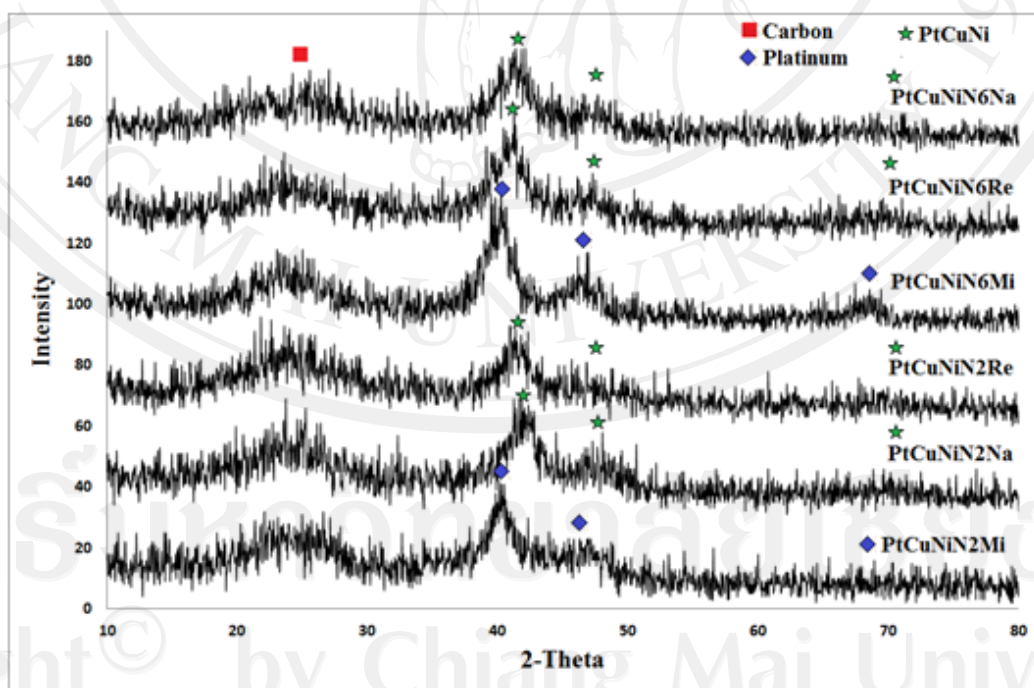


Figure 3.7 Powder XRD patterns of platinum-copper-nickel catalysts supported on treated carbon N115 by microwave, reflux and  $\text{NaBH}_4$  reduction methods.

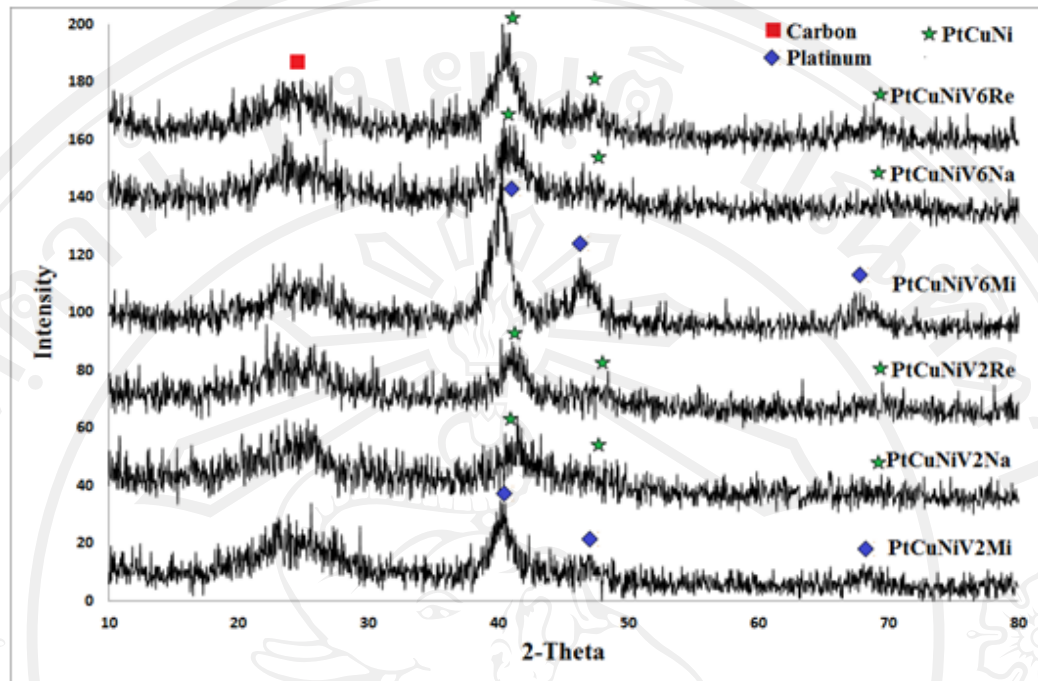


Figure 3.8 Powder XRD patterns of platinum-copper-nickel catalysts supported on treated carbon VulcanXC-72 by microwave, reflux and  $\text{NaBH}_4$  reduction methods.

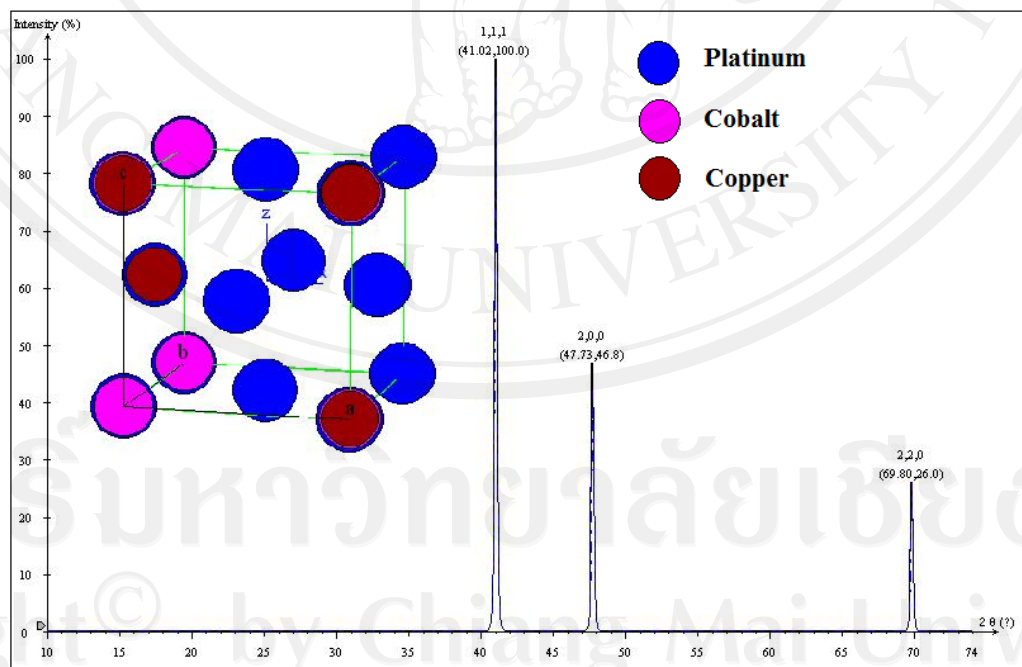


Figure 3.9 Simulated platinum-cobalt-copper unit cell by CaRIne V3.1 from Patent data No. 5,178,971 and XRD pattern.

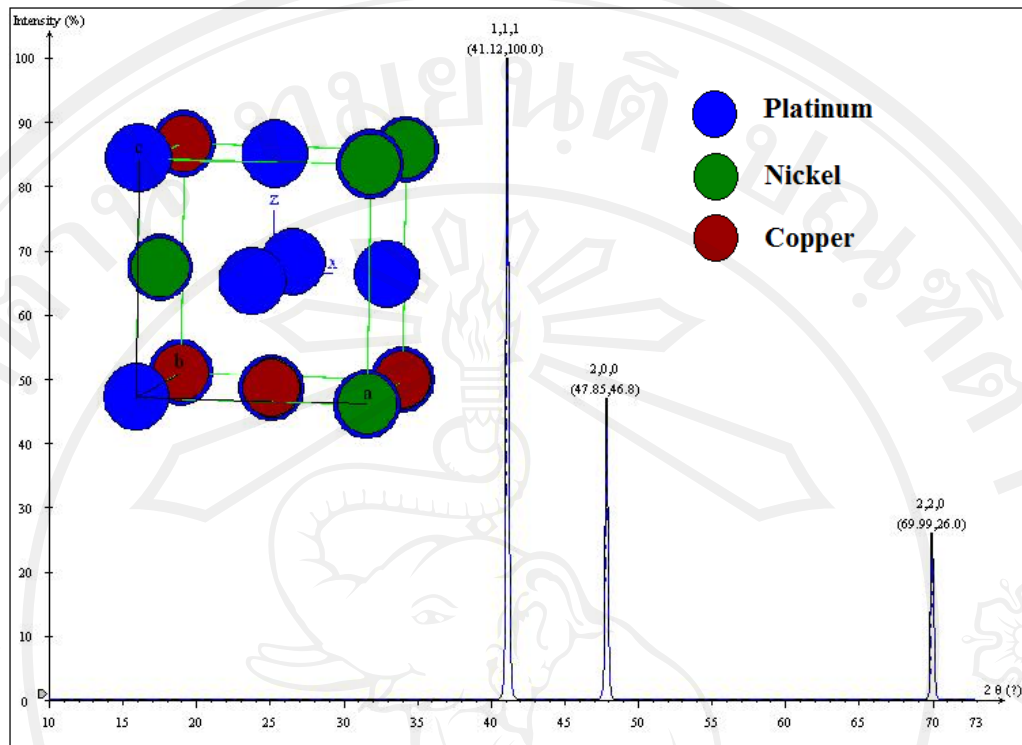


Figure 3.10 Simulated platinum-cobalt-nickel unit cell by CaRIne V3.1 from Patent data No. 5,178,971 and XRD pattern.

The XRD patterns for this research were separated into three groups which were 1). pattern without metal peak, 2). pattern with only platinum peak, and 3). pattern with ternary metal alloy peak.

First group, catalysts such as PtCoCrV<sub>2</sub>Na and PtCoCrVu<sub>2</sub>Na were counted as the metal phase unidentification because of low amount of metal and small particle size of metals. However, these catalysts were confirmed the existence of Pt-CoO-Cr<sub>2</sub>O<sub>3</sub> from SAD pattern of TEM and from XAS techniques. The reason for the formation of CoO and Cr<sub>2</sub>O<sub>3</sub> phase instead of cobalt and chromium metals was the cobalt ion (+2) and chromium ion (+3) were the most oxidation state under air atmosphere [85,86]

although the standard reduction potentials of both species were higher than  $\text{NaBH}_4$  ( $E^0_{\text{Co}} = -0.28$ ,  $E^0_{\text{Cr}} = -0.74$  and  $E^0_{\text{NaBH}_4} = -1.65$ ) [87,63].

Second group, the catalysts  $\text{PtCoCrV}_2\text{Mi}$ ,  $\text{PtCoCrVu}_2\text{Mi}$ ,  $\text{PtCoCrN}_2\text{Re}$ ,  $\text{PtCoFeN}_2\text{Re}$ ,  $\text{PtCoNiN}_2\text{Re}$ ,  $\text{PtCuNiN}_2\text{Mi}$ ,  $\text{PtCuNiN}_6\text{Mi}$ ,  $\text{PtCuNiV}_2\text{Mi}$ , and  $\text{PtCuNiV}_6\text{Mi}$  were identified and observed platinum as a major phase. For the sample  $\text{PtCoCrV}_2\text{Mi}$  and  $\text{PtCoCrVu}_2\text{Mi}$  catalysts, the absence of cobalt metal formation could be explained by the insufficient of microwave energy to support the reduction of  $\text{Co}^{2+}$  ion to cobalt metal while the absence of chromium metal  $\text{Cr}_2\text{O}_3$  (identify by XAS) was that because the chromium ion ( $\text{Cr}^{+3}$ ) is the most stable oxidation state [58]. It has a negative standard reduction potential and hence a high possibility to occur as an oxide [85,86]. For the samples from reflux method which were  $\text{PtCoCrN}_2\text{Re}$ ,  $\text{PtCoFeN}_2\text{Re}$ , and  $\text{PtCoNiN}_2\text{Re}$  catalysts, only platinum phase was found. Other metals which held negative standard reduction potentials ( $E^0_{\text{Co}} = -0.28$ ,  $E^0_{\text{Cr}} = -0.74$ ,  $E^0_{\text{Fe}} = -0.04$ , and  $E^0_{\text{Ni}} = -0.257$ ) [87], were stable in oxide formula. Finally, the sample  $\text{PtCuNiN}_2\text{Mi}$ ,  $\text{PtCuNiN}_6\text{Mi}$ ,  $\text{PtCuNiV}_2\text{Mi}$ , and  $\text{PtCuNiV}_6\text{Mi}$  catalysts, contained only platinum phase because alloy phase was unable to synthesize by microwave method where copper and nickel ions were favorable  $\text{CuO}$  [88,89] and  $\text{NiO}$  [90,91] phase by this method. The microwave which used in this study was low irradiation to reduce the metal ion to metal in air atmosphere.

Third group, the catalysts  $\text{PtCoCuN}_2\text{Re}$ ,  $\text{PtCuNiN}_2\text{Re}$ ,  $\text{PtCuNiN}_6\text{Re}$ ,  $\text{PtCuNiN}_2\text{Na}$ ,  $\text{PtCuNiN}_6\text{Na}$ ,  $\text{PtCuNiV}_2\text{Re}$ ,  $\text{PtCuNiV}_6\text{Re}$ ,  $\text{PtCuNiV}_2\text{Na}$ , and  $\text{PtCuNiV}_6\text{Na}$  were identified as platinum-based ternary catalysts. The unit cell from these catalysts was cubic and space group was  $\text{Fm}\bar{3}\text{m}$ . The  $2\theta$  position of (111) plane of sample was compared with platinum ternary alloy from Patent No. 5,178,971 and

platinum metal shown in Table 3.2. From PtCoCuNi<sub>2</sub>Re, the position of (111) plane was closer to platinum alloy's than platinum metal's because the unit cell from platinum alloy was smaller than platinum metal. This alloy was counted as substitutional alloy; metal was replaced by other metals at the same position. In this sample, cobalt and copper with the smaller atomic radius than platinum had replaced the platinum position. After the metals were mixed to form alloy, the acquired alloy phase provided the different unit cell parameters from the metal. In case of the atomic distance, the distance between the same atomic types appeared further than the distance from heteroatom by the effect of the atomic force. For the same reason, the position of (111) plane of PtCuNi alloy and PtCoCu alloy catalysts also appeared closer to platinum alloy's than platinum metal's.

The platinum-based ternary catalysts were the formation of platinum, copper and cobalt or nickel. These catalysts were prepared by reflux and NaBH<sub>4</sub> reduction methods. The reducing agent using reflux method was ethylene glycol and NaBH<sub>4</sub> reduction method was NaBH<sub>4</sub>. The reducing agent in these two methods had electrons that can donate to the metal ion. The alloy formation was explained in Figure 3.11. When metal ions approached near the carbon surface, the reducing agents gave the electron to metal ion which later grew on the carbon supporter.

For the sample contained platinum and copper had positive standard reduction potentials, so it was simple to be reduced. Nickel and cobalt, which held the negative standard reduction potentials as -0.257 and -0.28, respectively, were difficult to be reduced to metal. For PtCoCuNi<sub>2</sub>Re catalyst formed as alloy because of standard reduction potentials from platinum and copper were positive which simple to be

reduced by reducing agent. Solution contained metal ion (Pt, Cu and Co) as the positive charge near the carbon surface which was negative charge. When ethylene glycol was heated by reflux method, it reduced metal ion near the carbon surface to metal-alloy. The platinum and copper ions were easier to be reduced than other metal when all metal ions were close to the carbon surface. The ethylene glycol at 170 °C can reduce platinum, copper and cobalt ions to form PtCoCu alloy. These sample PtCuNiN2Re, PtCuNiN6Re, PtCuNiV2Re, and PtCuNiV6Re were prepared by reflux method while the sample PtCuNiN2Na, PtCuNiN6Na, PtCuNiV2Na, and PtCuNiV6Na were prepared by NaBH<sub>4</sub> reduction method. The results from these catalysts appeared similarly as the result from sample PtCoCuN2Re catalysts which the alloy phase was found except the sample from NaBH<sub>4</sub> reduction method which used NaBH<sub>4</sub> as a reducing agent.

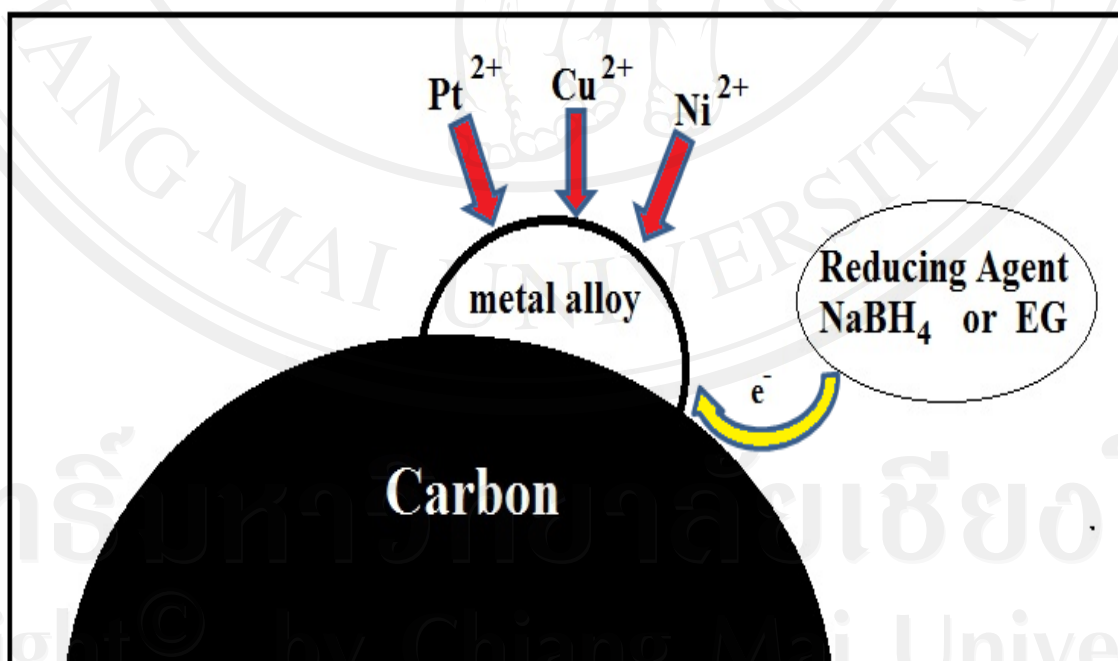


Figure 3.11 The formation of platinum alloy by reducing agent

Table 3.2 Compared peak position of (111) between standard and sample with unit cell parameters. (\* from JCPDS No. 00-004-0802, \*\* from Patent No. 5,178,971)

Sample	2 $\theta$ (111)	a(Å)
Pt STD*	39.76	3.920
PtCoCu STD**	41.02	3.808
PtCuNi STD**	41.12	3.799
PtCuNiN2Na	41.64	3.752
PtCuNiN6Na	41.24	3.787
PtCuNiV2Na	41.40	3.773
PtCuNiV6Na	40.88	3.819
PtCoCuN2Re	40.93	3.810
PtCuNiN2Re	41.00	3.808
PtCuNiN6Re	41.16	3.794
PtCuNiV2Re	41.04	3.805
PtCuNiV6Re	40.76	3.830

### 3.2.2 Scanning electron microscopy (SEM) and energy dispersive spectroscopy (EDS)

The catalysts for all group characterized by SEM technique was shown in Figure 3.12-3.14. The Figure 3.12 showed catalyst in the first group which only carbon surface of carbon Vulcan XC-72 was observed because the supported metals had very fine particle which was beyond the detection limit of this technique. Their

particle size distribution and morphologies were further investigated by TEM. For Figure 3.12- 3.14, the catalysts in second and third groups were presented, respectively. The results were similar to the catalysts in the first group that only the surfaces of carbon Vulcan XC-72 and carbon N115 were observed.

The qualitative and quantitative analyses of elements for all samples were conducted by EDS technique as shown in Table 3.3- 3.5. The intensities of EDS peaks of carbon, oxygen and all metals on carbon were presented. The observed oxygen from this technique was majorly come from carboxylic group on treated carbon surface. The comparison of metal amount on treated carbon and untreated carbon was demonstrated in Table 3.3 where all metals (Pt, Co and Cr) were found on both carbon supporters. However, there was no evidence of cobalt metal occurrence on both carbon supporters from microwave method. The reason for the absence of cobalt metal can be explained by the insufficient of microwave energy to support the reduction of  $\text{Co}^{2+}$  ion to Co metal. It was noted that the intensities of EDS spectrums, which corresponded to higher amount of all metals on treated carbon were higher than the metals on untreated carbon. The quantitative analysis from EDS spectrum showed that the metals on treated carbon were relatively higher than on untreated carbon. For Table 3.4-3.5, the elemental amounts contained in each catalyst from second and third groups, were presented, respectively. All metals supported on carbon, however, the amount of the observed metals was less than theoretical metals ratio.

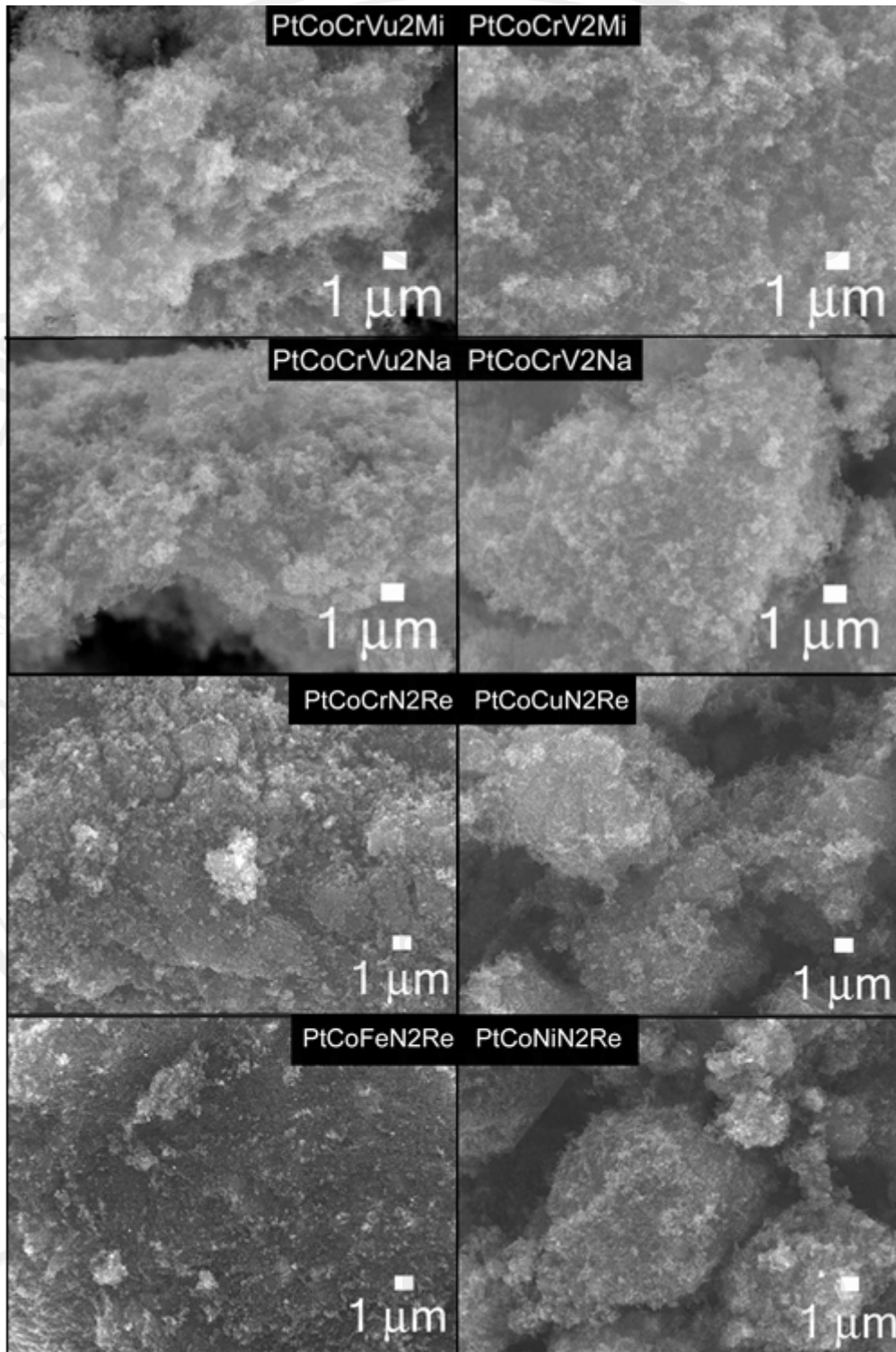


Figure 3.12 SEM pictures of platinum-cobalt-chromium catalysts supported on treated or untreated carbons by microwave and  $\text{NaBH}_4$  reduction method and platinum-cobalt-metal catalysts supported on treated carbon by reflux method.

Table 3.3 Percent weights of platinum, cobalt, chromium, oxygen and carbon of platinum-based ternary catalysts from EDS.

Sample	Element (Wt %)				
	C	O	Pt	Co	Cr
PtCoCrVu2Mi	87.35	7.99	3.51	0.04	1.11
PtCoCrVu2Na	86.60	5.51	5.28	1.73	0.88
PtCoCrV2Mi	85.98	6.17	5.63	0.00	2.22
PtCoCrV2Na	82.71	5.18	6.65	3.38	2.08

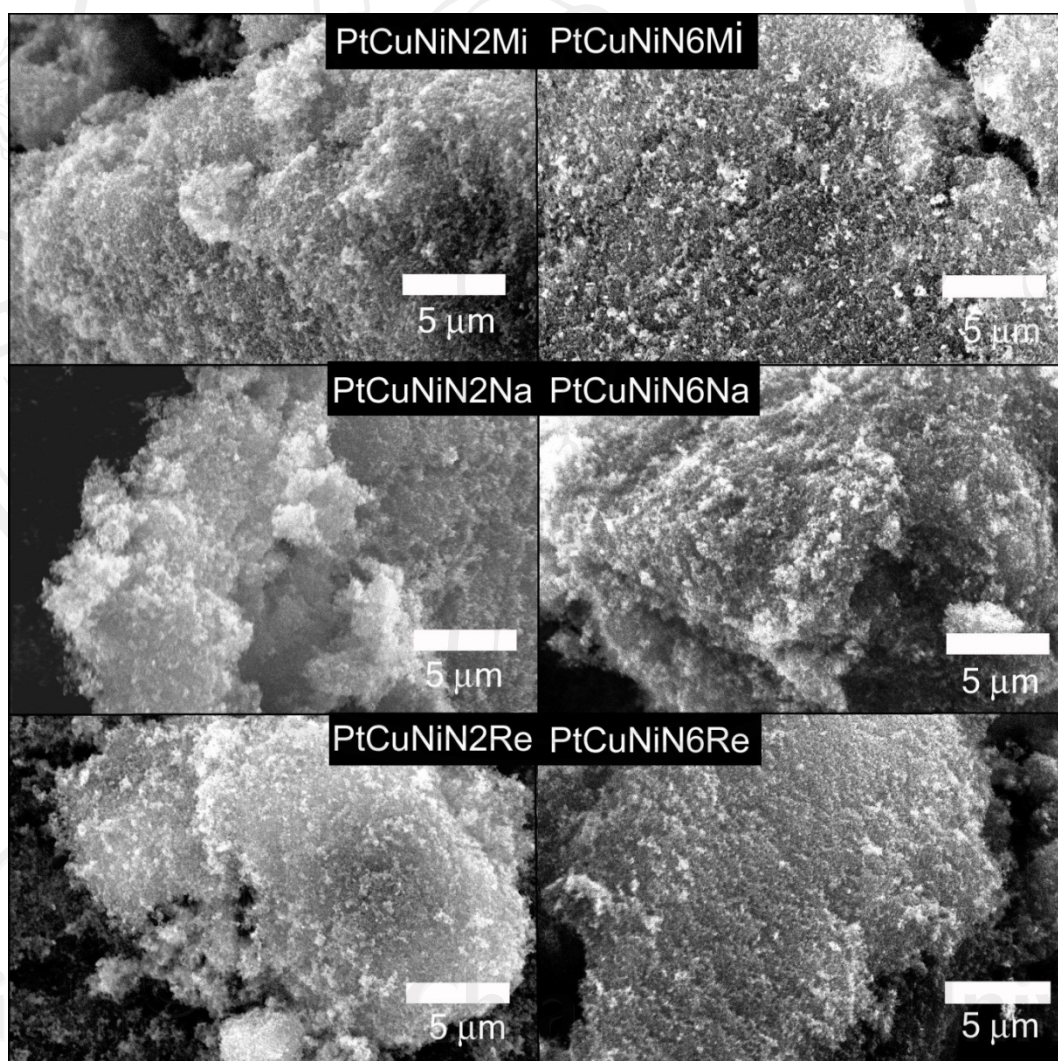


Figure 3.13 SEM pictures of platinum-copper-nickel catalysts supported on treated carbon N115 by microwave, reflux and  $\text{NaBH}_4$  reduction methods.

Table 3.4 Percent weights of platinum, cobalt, metals(chromium, copper, nickel, and iron), oxygen and carbon of platinum-based ternary catalyst from EDS.

Sample	Element (Wt %)				
	C	O	Pt	Co	M
PtCoCrN2Re	74.52	11.68	10.06	1.29	2.46
PtCoCuN2Re	78.17	6.08	10.28	0.17	5.30
PtCoFeN2Re	76.20	9.59	11.38	1.22	1.30
PtCoNiN2Re	73.55	11.21	8.50	1.17	5.57

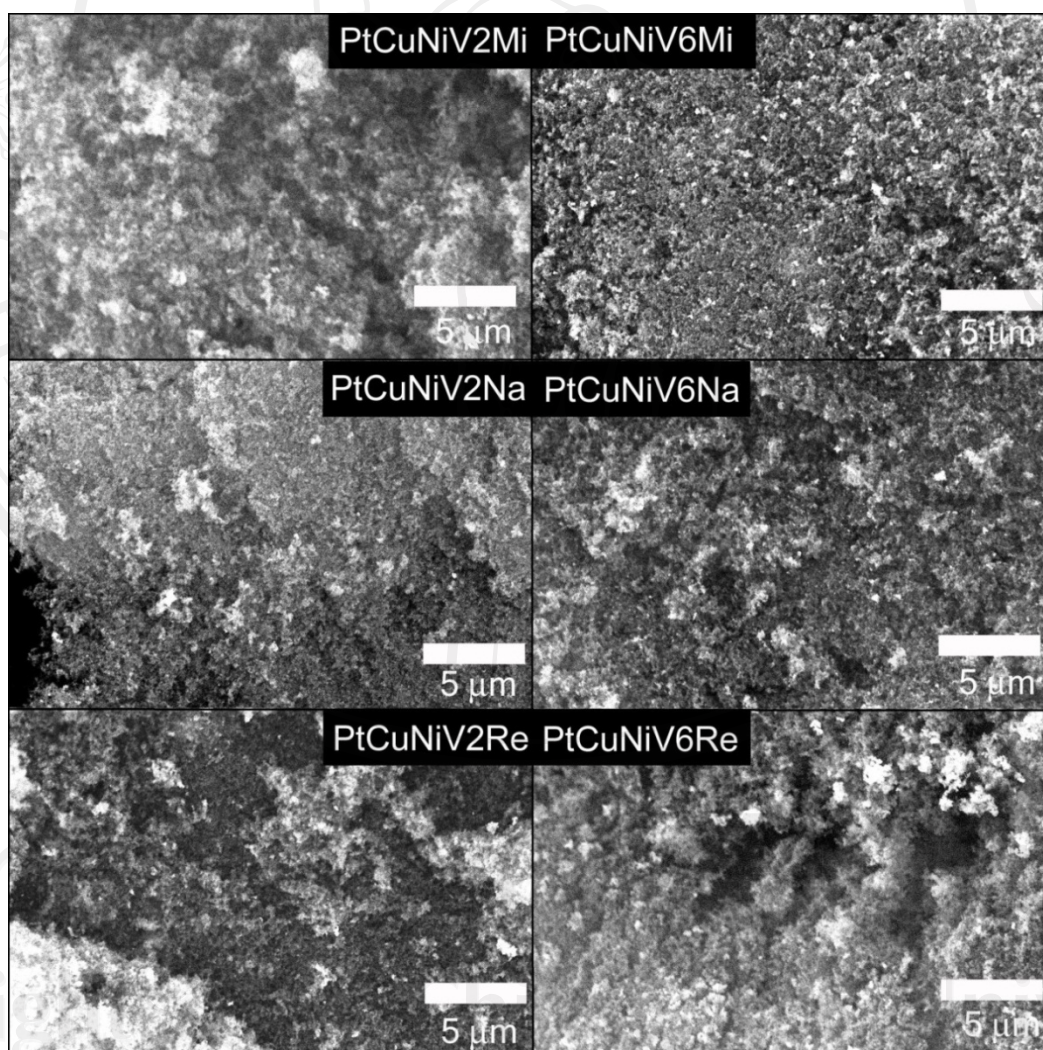


Figure 3.14 SEM pictures of platinum-copper-nickel catalysts supported on treated carbon VulcanXC-72 by microwave, reflux and  $\text{NaBH}_4$  reduction methods.

Table 3.5 Percent weights of platinum, copper, nickel, oxygen and carbon of platinum-based ternary catalyst from EDS.

Sample	Element (Wt %)				
	C	O	Pt	Cu	Ni
PtCuNiN2Mi	74.07	10.87	7.35	5.52	2.19
PtCuNiN2Na	75.07	12.79	5.32	4.46	2.16
PtCuNiN2Re	74.42	9.46	8.40	4.81	2.92
PtCuNiN6Mi	78.64	9.52	10.17	1.55	0.27
PtCuNiN6Na	74.65	9.52	10.17	1.55	0.27
PtCuNiN6Re	75.72	6.93	12.34	2.45	2.56
PtCuNiV2Mi	82.27	9.02	7.18	1.47	0.22
PtCuNiV2Na	80.11	7.08	7.39	5.05	0.56
PtCuNiV2Re	79.31	3.74	12.79	3.71	0.42
PtCuNiV6Mi	83.37	4.48	10.57	1.51	0.28
PtCuNiV6Na	81.35	5.55	9.37	2.72	1.02
PtCuNiV6Re	77.66	9.74	10.32	2.18	0.29

### 3.2.3 Transmission electron microscopy (TEM)

The TEM images of catalyst on untreated and treated carbons for microwave and  $\text{NaBH}_4$  reduction methods were shown in Figure 3.15. It was found that the catalysts were nanoparticles with a good dispersion on carbon surface. The average particle size was shown in Table 3.6 and Figure 3.16. The particle size histograms were shown in Figure 3.17. The results showed that particle size of catalysts on treated carbon was smaller than the catalyst particles on untreated carbon for both methods. The smaller particle size was possibly influenced by the carboxylic group on carbon surface which had negative charge. Therefore, they absorbed metal ions to near carbon surface and diffused metal ion to all surface. In general, the catalyst with a good uniform by

distribution of nanoscales particles will improve the fuel cell performance due to high surface area. The selected area electron diffraction (SAD) patterns for the catalysts in this group were inserted in TEM images. From  $\text{NaBH}_4$  reduction method, the diffracted ring patterns of (002), (101) and (102) planes of carbon and (111), (200) and (220) planes of platinum were identified. For microwave method, the ring patterns contained (002), (101) and (102) planes for both carbons were obtained. In addition, spot pattern of platinum, which corresponded to (1-11), (-111) and (002) planes, was found for the catalyst on untreated carbon while only (1-11) plane of platinum was observed for the catalyst with treated carbon. It was confirmed that the catalysts in this group had platinum as the major phase. Other metals (cobalt and chromium) were not appeared in SAD patterns in this technique.

Table 3.6 Average particle size of all catalysts in this research

Sample	Particle size (nm)	Sample	Particle size (nm)
PtCoCrVu2Mi	2.72±0.41	PtCoCrN2Re	3.55±0.90
PtCoCrV2Mi	2.43±0.34	PtCoCuN2Re	4.09±0.69
PtCuNiN2Mi	3.14±0.52	PtCoFeN2Re	3.22±0.60
PtCuNiN6Mi	3.26±0.65	PtCoNiN2Re	3.28±0.47
PtCuNiV2Mi	3.17±0.66	PtCuNiN2Re	3.16±0.55
PtCuNiV6Mi	4.41±0.74	PtCuNiN6Re	3.46±0.88
PtCoCrVu2Na	2.97±0.63	PtCuNiV2Re	3.51±0.58
PtCoCrV2Na	1.93±0.35	PtCuNiV6Re	3.96±0.67
PtCuNiN2Na	2.81±0.52	PtCuNiV2Na	2.78±0.70
PtCuNiN6Na	2.75±0.56	PtCuNiV6Na	2.73±0.55

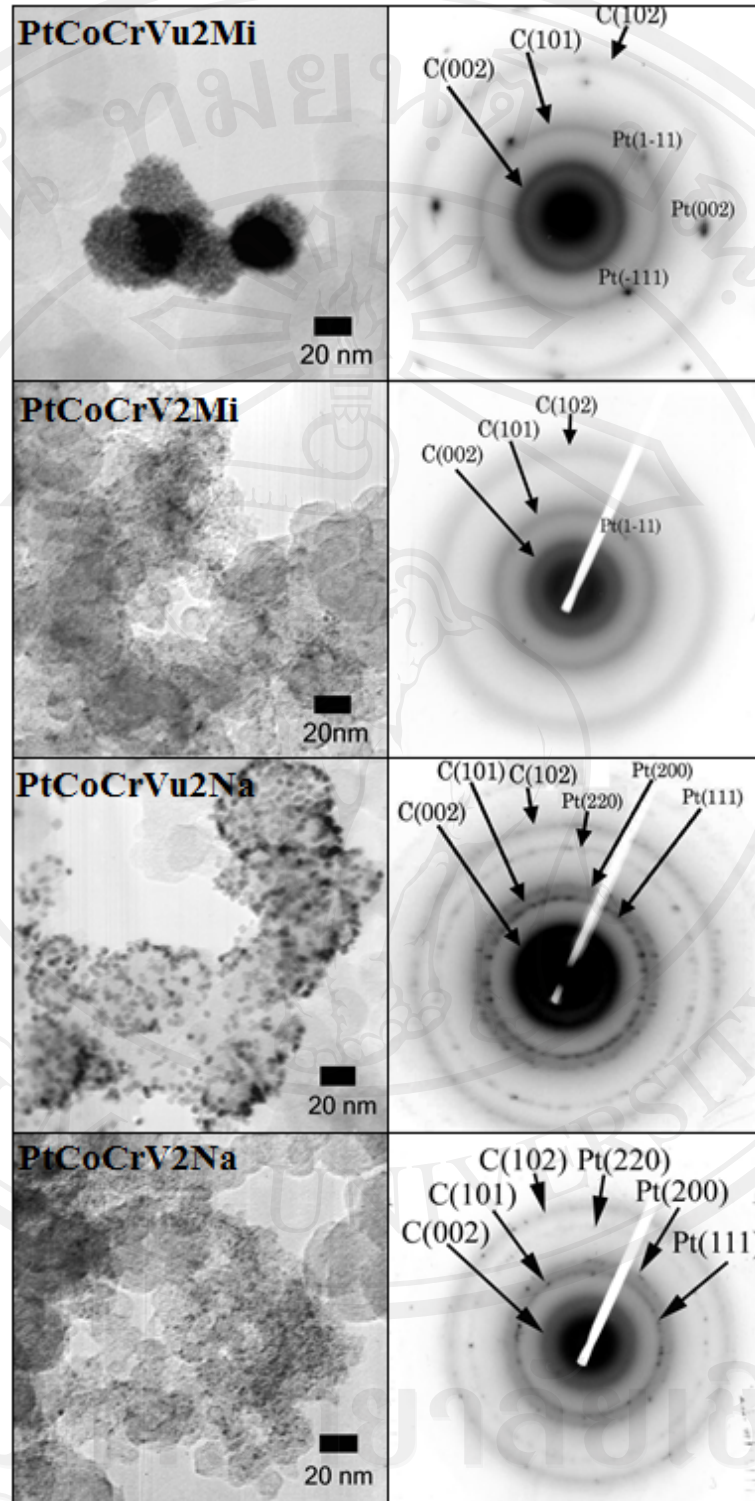


Figure 3.15 TEM images with the corresponding SAD patterns of platinum-cobalt-chromium catalysts supported on treated or untreated carbon by microwave and  $\text{NaBH}_4$  reduction methods.

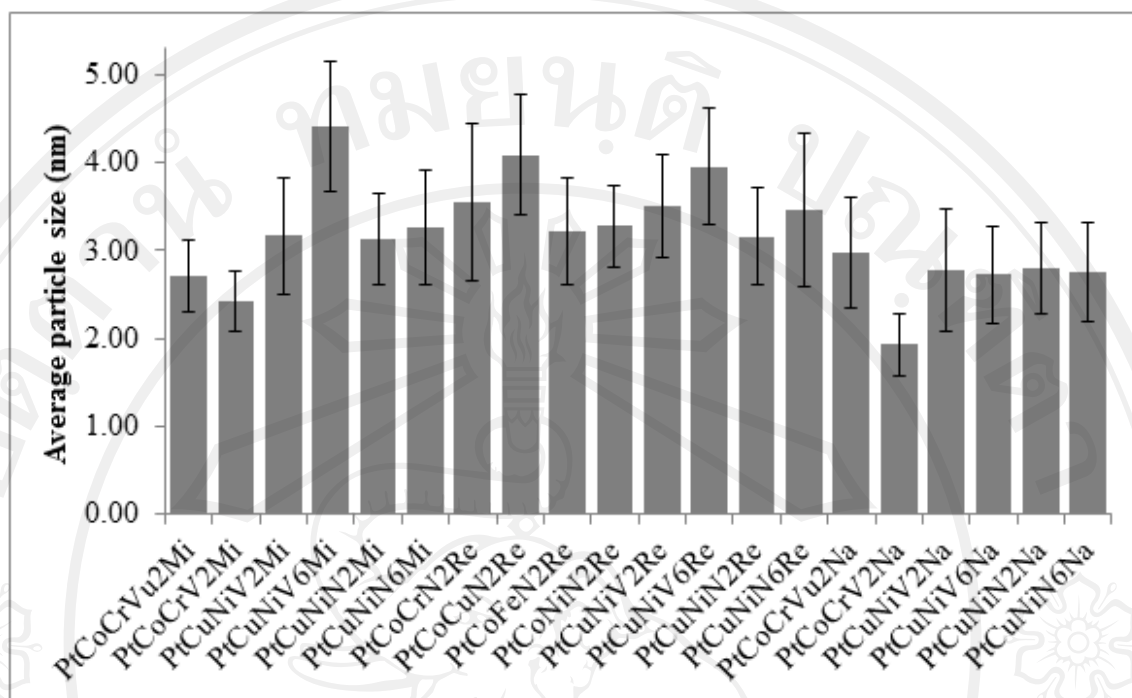


Figure 3.16 Average particle size of all catalysts in this research

Figure 3.18-3.22 shows the TEM images with the corresponding SAD patterns of catalysts on treated carbon supporter from second and third groups. It was found that the catalysts were nanoparticles with a good dispersion on carbon surface. The average particle size was shown in Table 3.6 and Figure 3.16. The particle size histograms were shown in Figure 3.23-3.25. The catalysts prepared by  $\text{NaBH}_4$  reduction method had smaller size than the catalysts from microwave and reflux methods.

SAD patterns of all samples from second and third groups were appeared as ring patterns which contained (002), (101) and (102) planes of carbon. The PtCoCrN2Re, PtCoFeN2Re, PtCoNiN2Re, PtCuNiN2Mi, PtCuNiN6Mi, PtCuNiV2Mi, and PtCuNiV6Mi contained (111), (200) and (220) planes of platinum. However, these catalysts contained all metals on carbon observed by EDS technique. The PtCoCuN2Re show the ring pattern contained (111), (200) and (220)

planes of platinum-cobalt-copper alloy. The PtCuNiN2Re, PtCuNiN6Re, PtCuNiN2Na, PtCuNiN6Na PtCuNiV2Re, PtCuNiV6Re, PtCuNiV2Na, and PtCuNiV6Na show the ring pattern contained (111), (200) and (220) planes of platinum-copper-nickel alloy. The SAD result was consistency with the results from XRD technique.

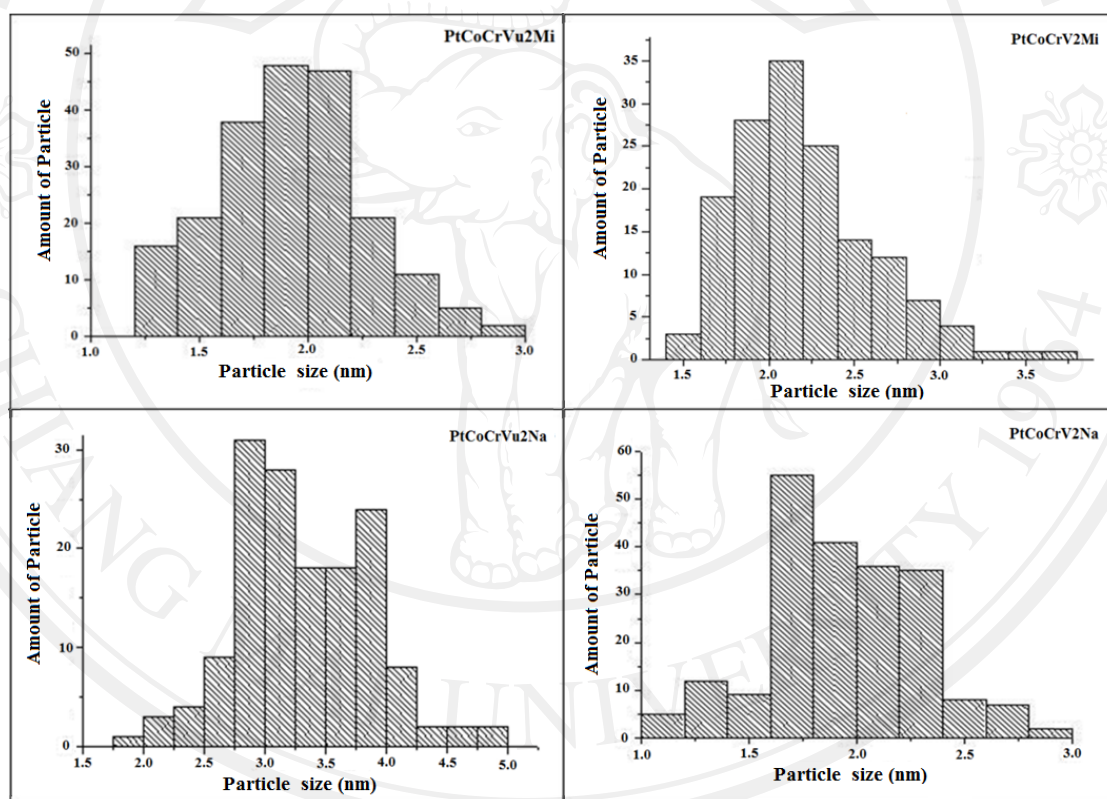


Figure 3.17 Particle size histograms of platinum-cobalt-chromium catalysts supported on treated or untreated carbon by microwave and NaBH<sub>4</sub> reduction methods.

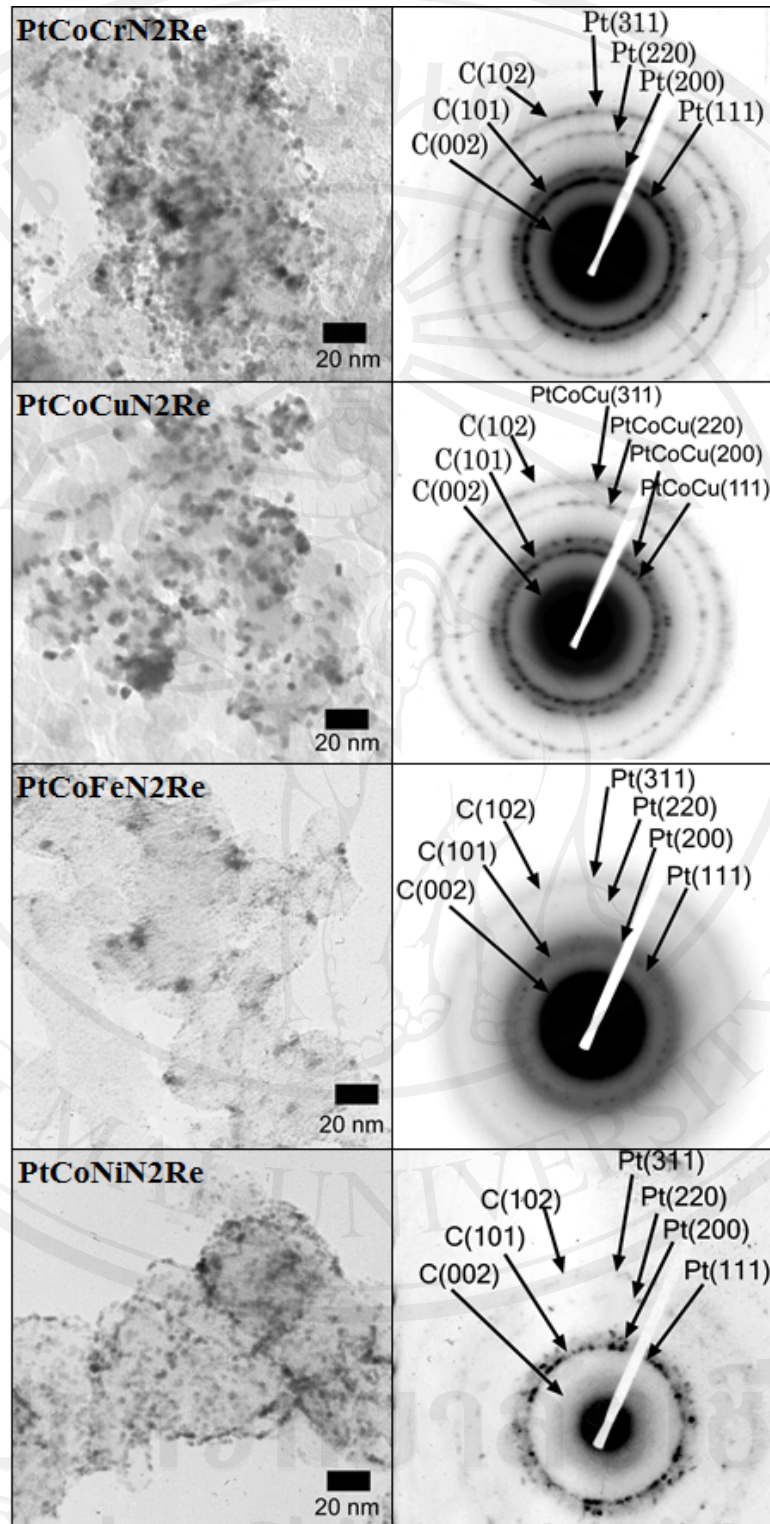


Figure 3.18 TEM images with the corresponding SAD patterns of platinum-cobalt-metal (metal = chromium, copper, iron, and nickel) catalysts supported on treated carbon by reflux method.

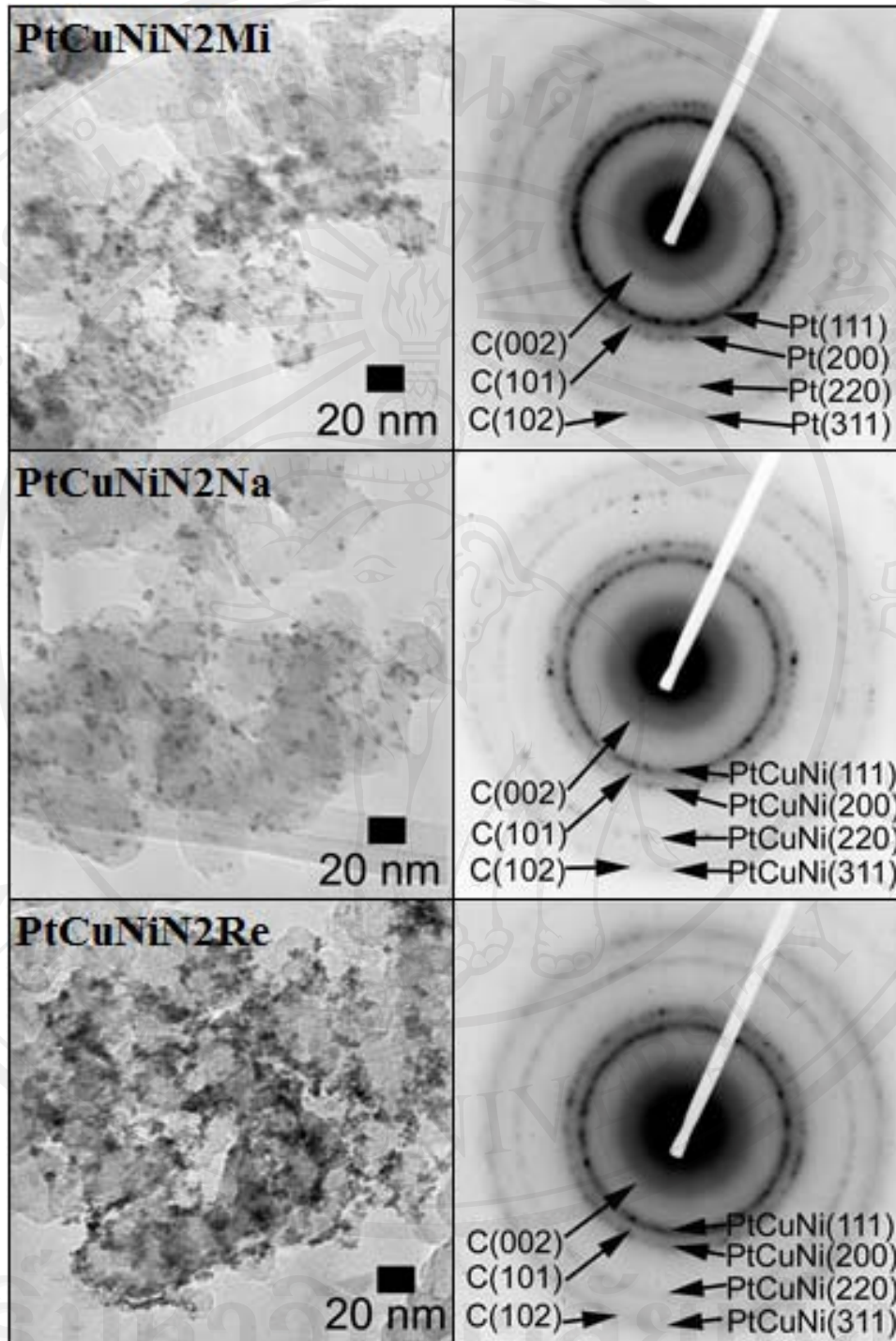


Figure 3.19 TEM images with the corresponding SAD patterns of platinum-copper-nickel catalysts ratio 2:1:1 supported on treated carbon N115 by microwave, reflux and NaBH<sub>4</sub> reduction method.

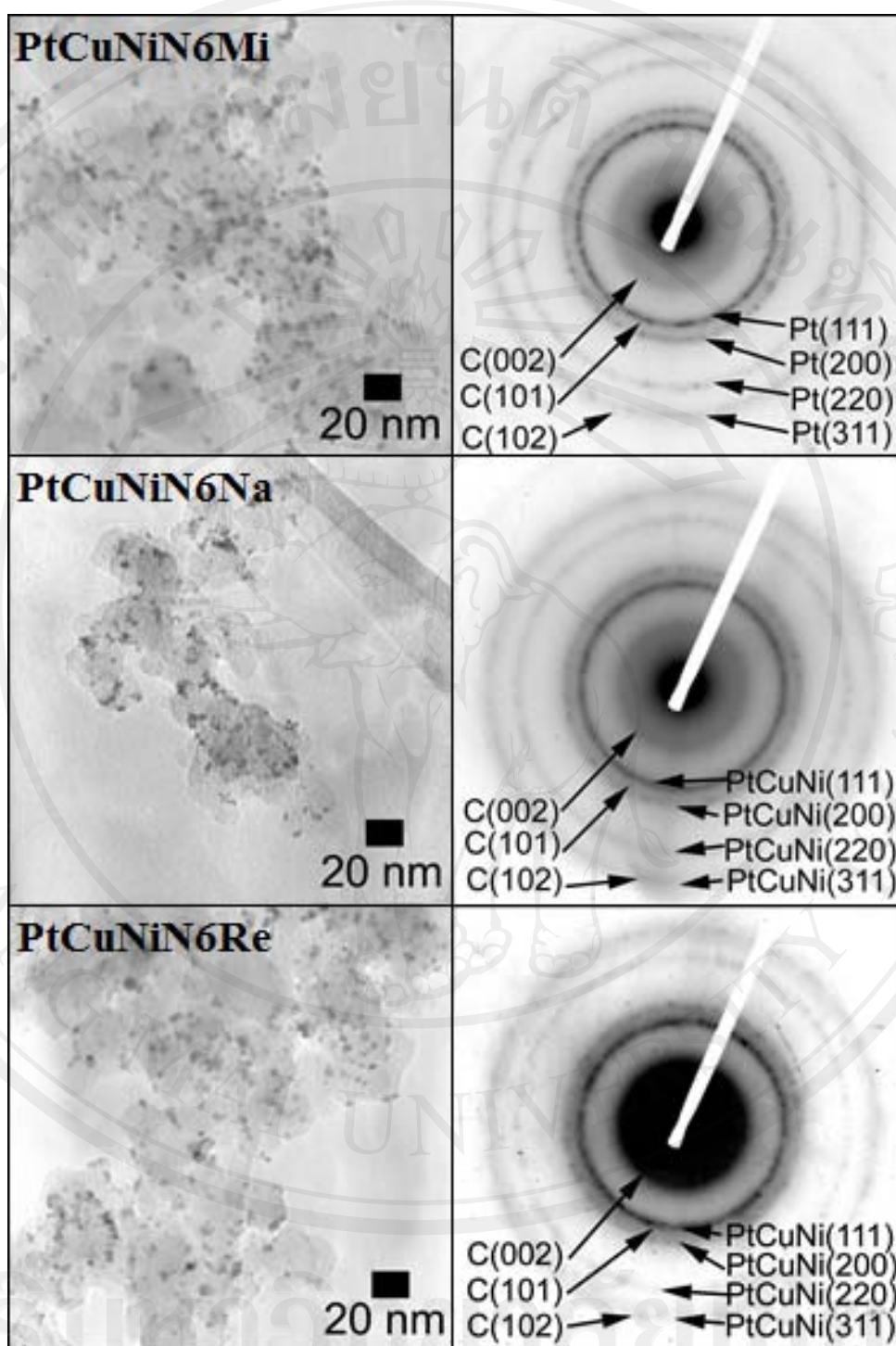


Figure 3.20 TEM images with the corresponding SAD patterns of platinum-copper-nickel catalysts ratio 6:1:1 supported on treated carbon N115 by microwave, reflux and  $\text{NaBH}_4$  reduction method.

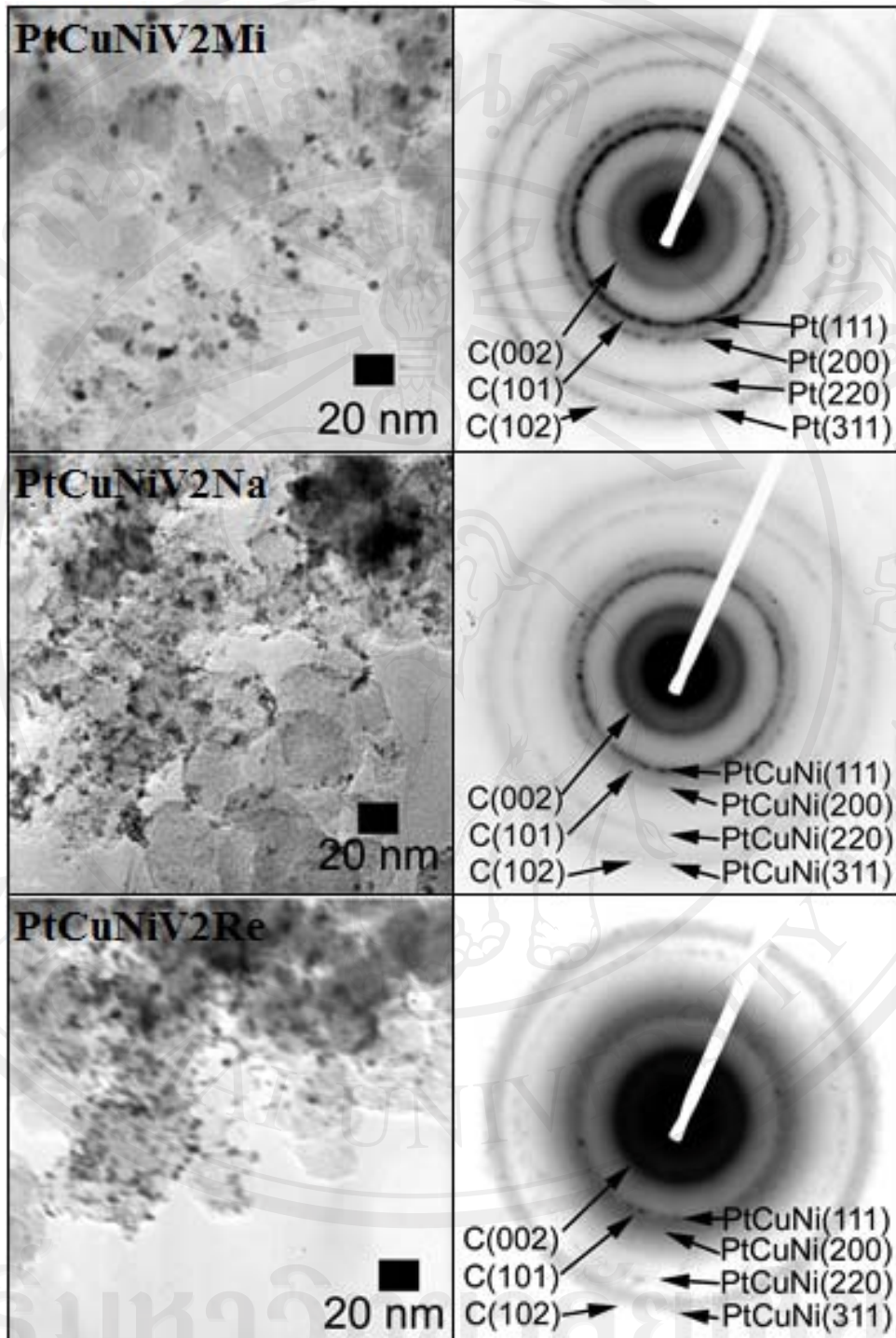


Figure 3.21 TEM images with the corresponding SAD patterns of platinum-copper-nickel catalysts ratio 2:1:1 supported on treated carbon VulcanXC-72 by microwave, reflux and  $\text{NaBH}_4$  reduction method.

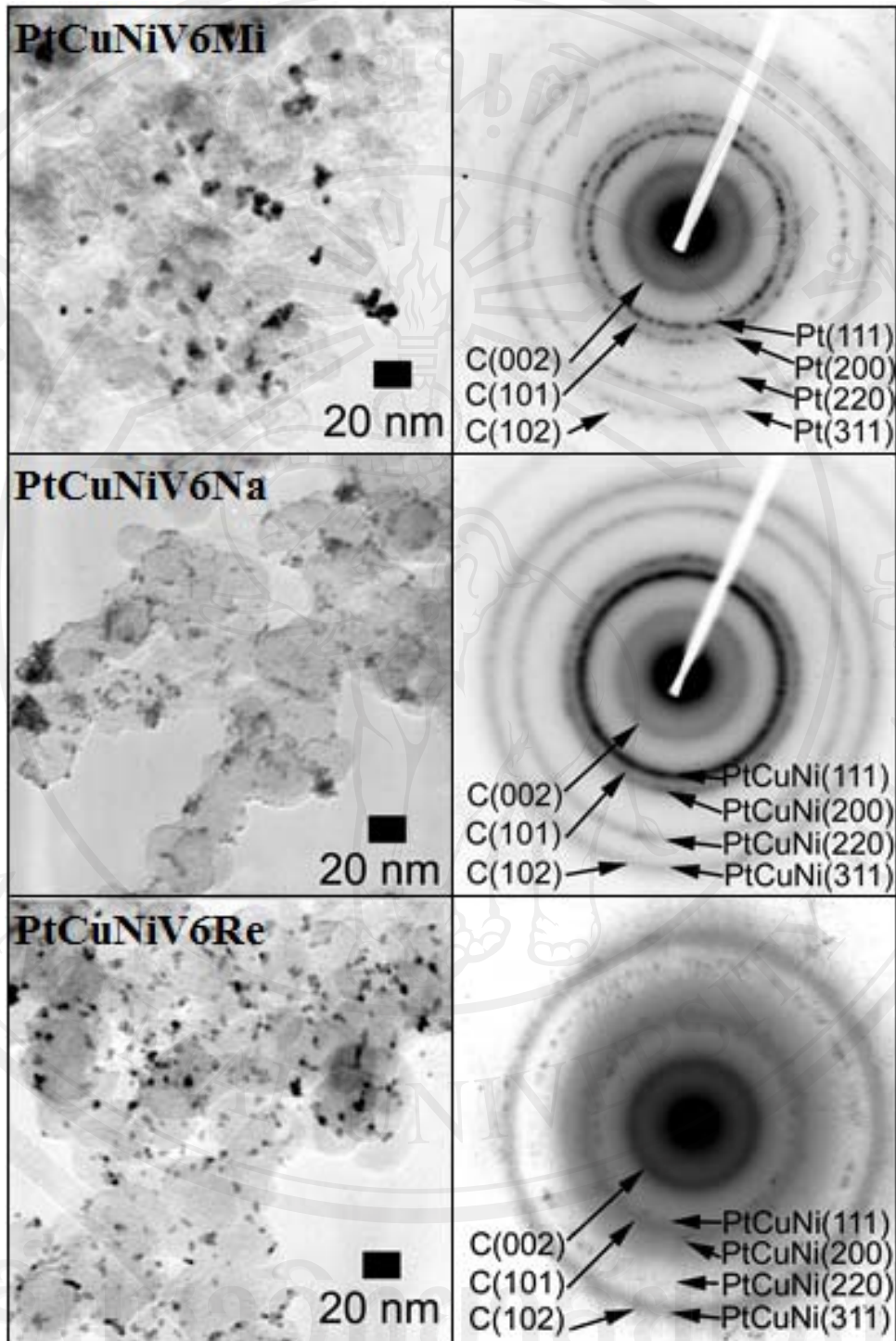


Figure 3.22 TEM images with the corresponding SAD patterns of platinum-copper-nickel catalysts ratio 6:1:1 supported on treated carbon VulcanXC-72 by microwave, reflux and  $\text{NaBH}_4$  reduction method.

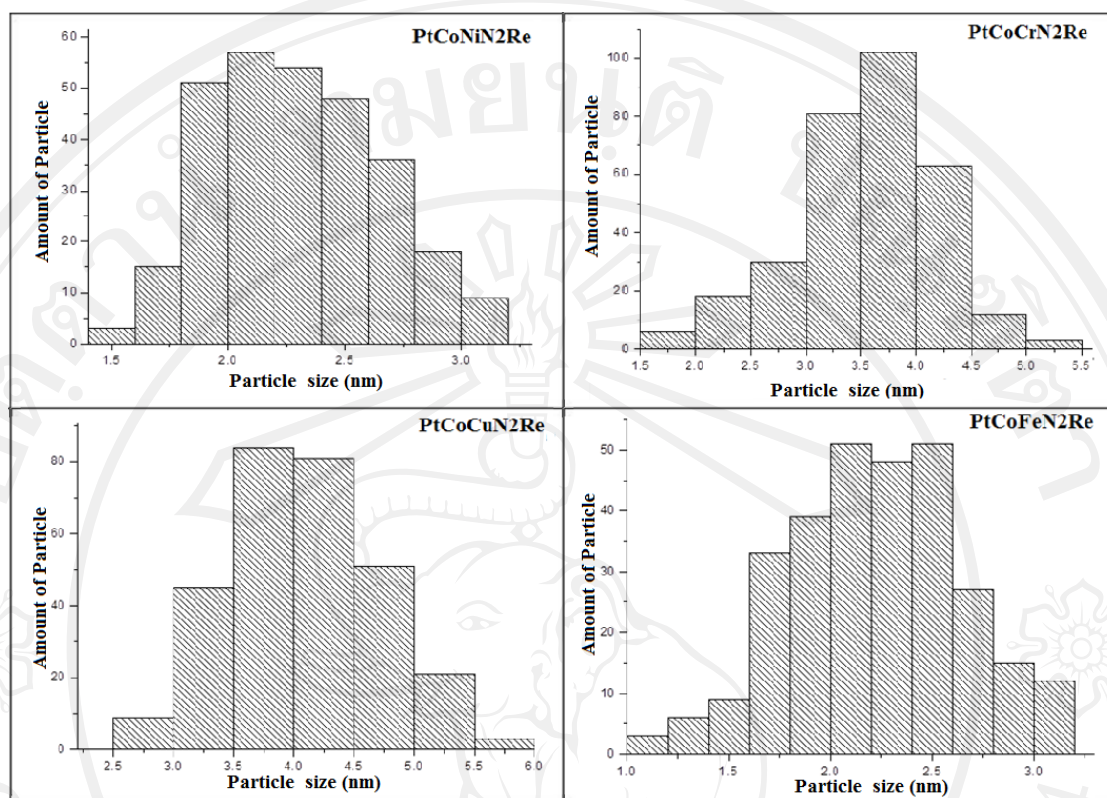


Figure 3.23 Particle size histograms of platinum-cobalt-metal catalysts supported on treated carbon by reflux method.

### 3.2.4 X-ray absorption spectrometry (XAS)

The XAS technique was used to identify formative phases of catalyst in the first group because some metal phase could not be observed by XRD technique. This technique used Co, CoO and Co<sub>3</sub>O<sub>4</sub> as cobalt standards and Cr and Cr<sub>2</sub>O<sub>3</sub> as chromium standards to compare with samples. The XANES and EXAFS spectra for sample and cobalt standards were shown in Figure 3.26. It confirmed that cobalt-contained phase in the samples obtained from NaBH<sub>4</sub> reduction method was CoO compound because of the similarity of characteristic spectra of CoO standard and sample. Conversely, there were no signals from cobalt-contained phase from samples which prepared by

microwave method. This result well agreed with the results from EDS and XRD technique.

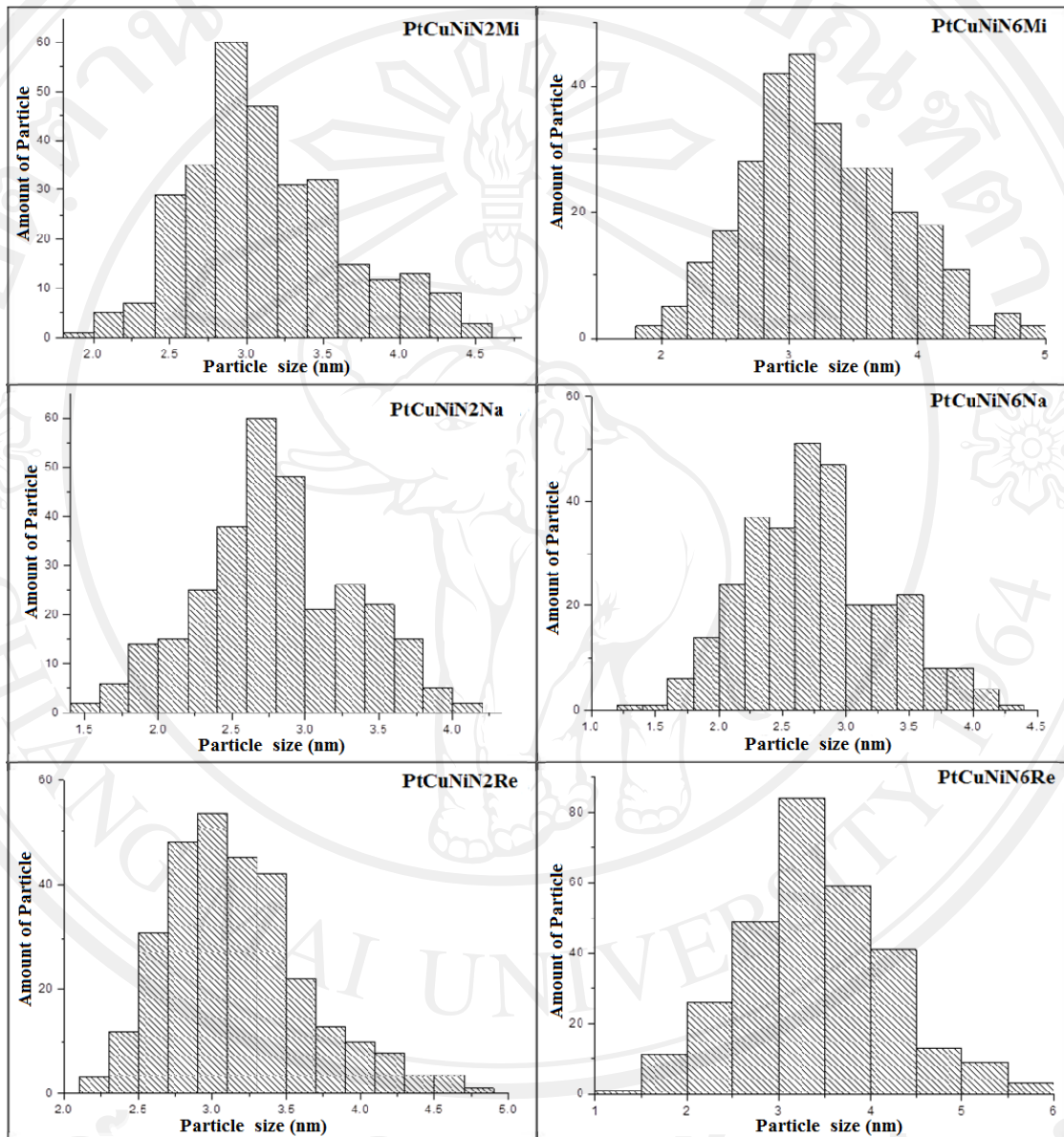


Figure 3.24 Particle size histograms of platinum-copper-nickel catalysts supported on treated carbon N115 by microwave, reflux and NaBH<sub>4</sub> reduction methods.

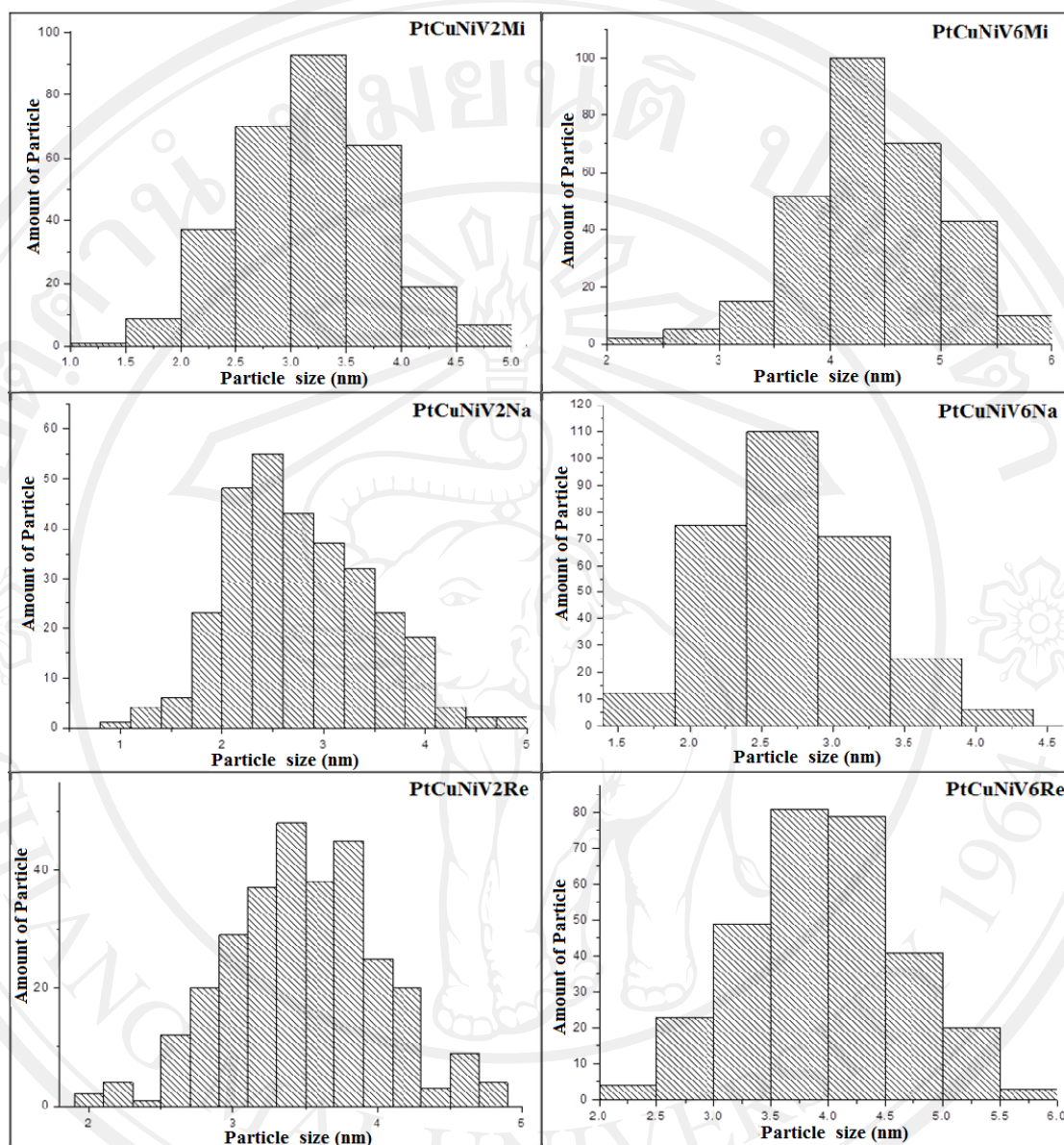


Figure 3.25 Particle size histograms of platinum-copper-nickel catalysts supported on treated carbon Vulcan XC-72 by microwave, reflux and  $\text{NaBH}_4$  reduction methods.

Figure 3.27 shows the XANES and EXAFS spectra of samples and chromium standards. All samples showed spectra which were similar to the spectrum of  $\text{Cr}_2\text{O}_3$  standard. It can be concluded that chromium-contained phase in the sample was  $\text{Cr}_2\text{O}_3$  compound. The existence of oxide phase can be explained by the preferable

oxidation state as chromium ion (+3) and cobalt ion (+2) for the preparation process which conducted in air atmosphere.

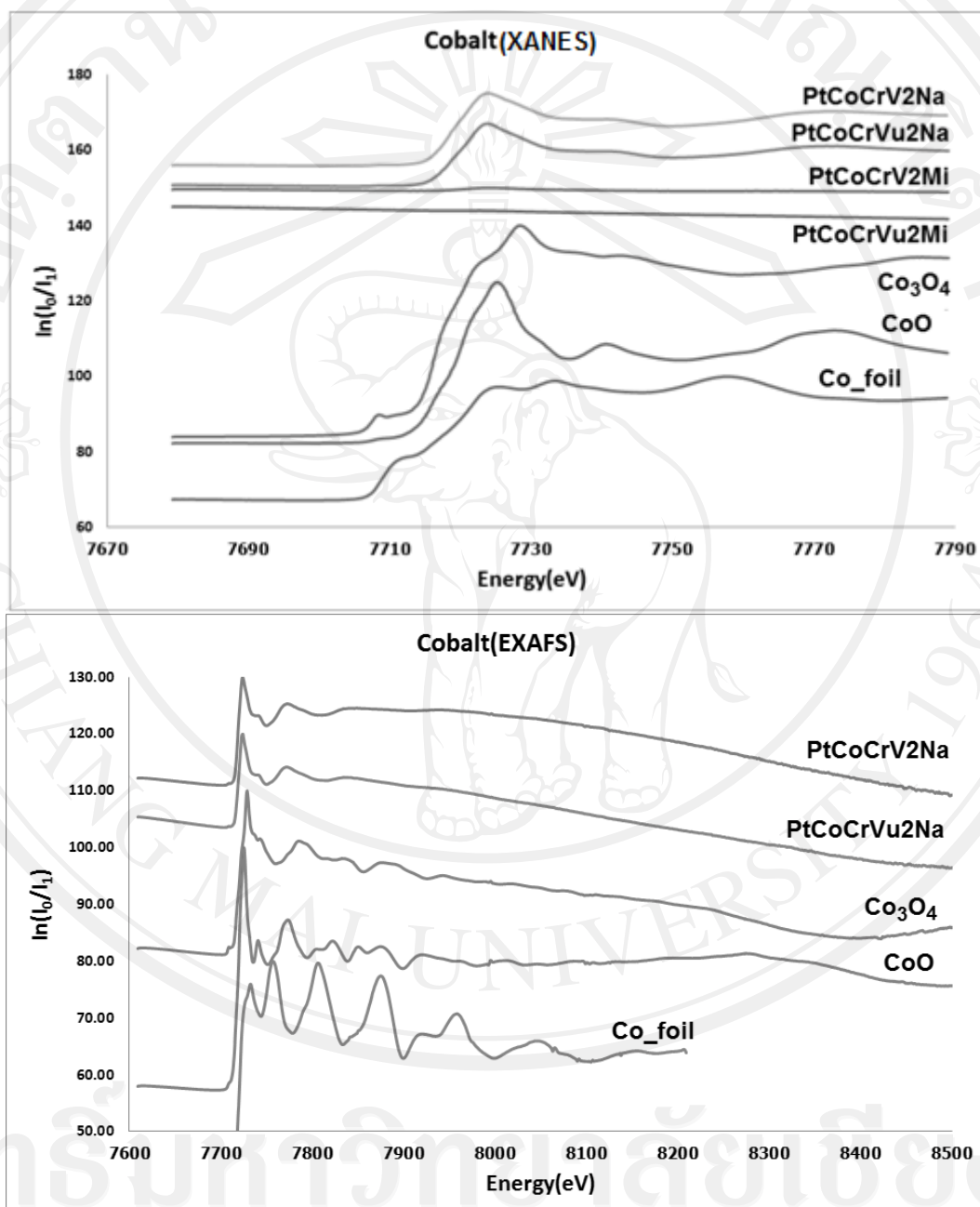


Figure 3.26 The XANES and EXAFS spectra of cobalt from catalysts supported on treated or untreated carbon by microwave and NaBH<sub>4</sub> reduction method compared with standard spectra of metal and metal oxides.

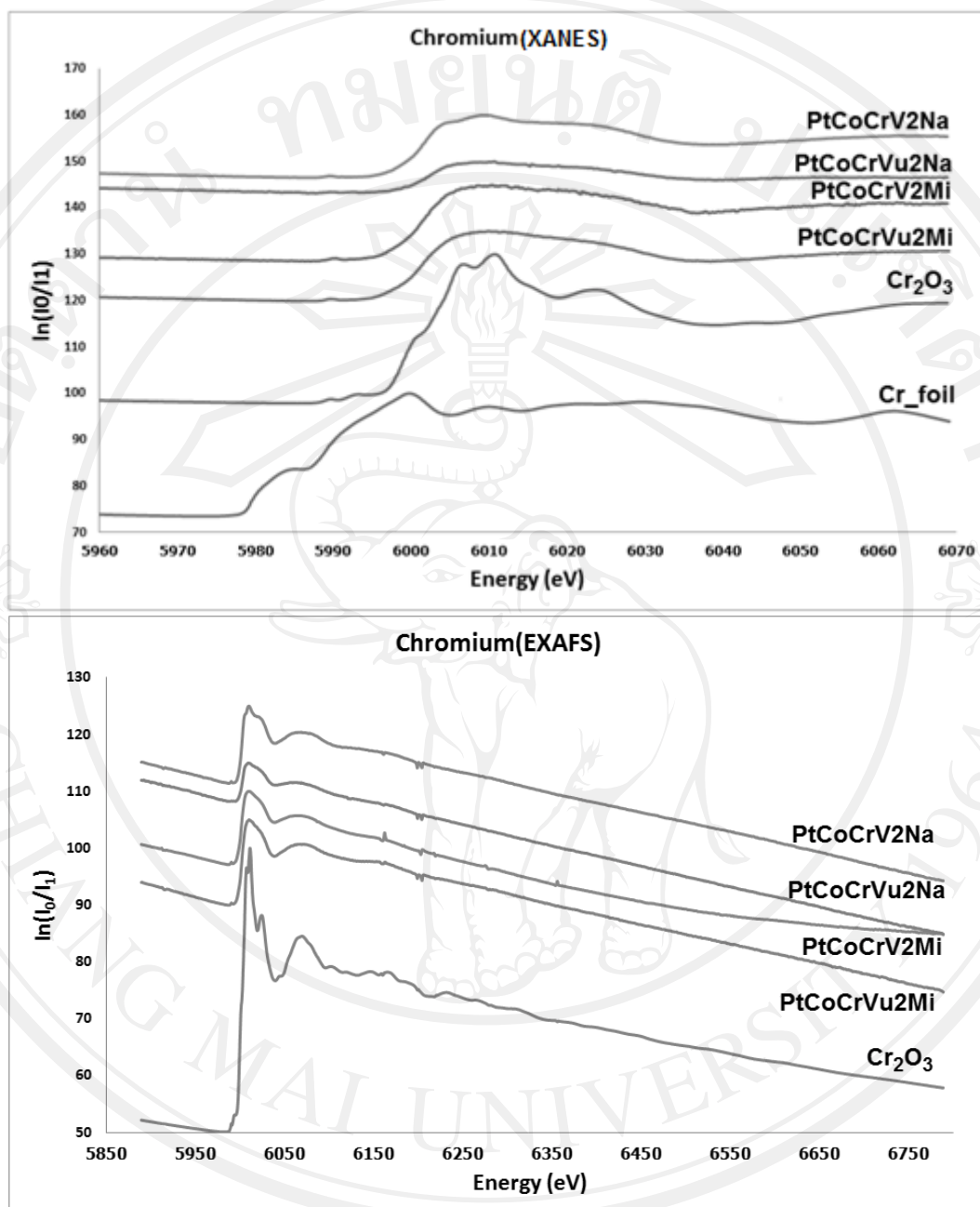


Figure 3.27 The XANES and EXAFS spectra of chromium from catalysts supported on treated or untreated carbon by microwave and NaBH<sub>4</sub> reduction method compared with standard spectra of metal and metal oxides.

### 3.2.5 Cyclic voltammetry (CV)

The electroactivities testing of the first group catalyst was investigated by CV. The comparison of voltammograms between the first group catalyst and commercial Pt/C catalyst from Fuel Cells Scientific was performed. The CV spectrums are shown in Figure 3.28. The maximum potential, current from reduction reaction and % weight ratio were shown in Table 3.7. It can be seen that all platinum-based ternary catalysts delivered higher current than commercial Pt/C when normalized by gram of platinum loading (weight calculation from EDS data). The PtCoCrV2Na showed highest current when compared the commercial Pt/C and PtCoCrV2Na, it was found that PtCoCrV2Na gave 2 times higher current than commercial Pt/C. This catalyst shown highest performance because of the particle size for this catalyst was smaller than other catalysts in first group (shown in Table 3.6), particle from this catalyst was well dispersed on treated carbon surface than particle on untreated carbon (shown in Figure 3.15) and this catalyst appeared ternary catalyst, Pt-CoO-Cr<sub>2</sub>O<sub>3</sub> (from XAS result). It can be concluded that the Pt-CoO-Cr<sub>2</sub>O<sub>3</sub> ternary catalyst supported on treated carbon prepared by NaBH<sub>4</sub> reduction method provided relatively higher potential than commercial catalyst. However, PtCoCrV2Na was confirmed by XAS to contain no platinum alloy catalyst. For this reason, this catalyst wasn't further tested the performance by single cell testing.

Table 3.7 Maximum potential and current from reduction reaction.

Sample	Potential (V)	Current (A/g <sub>Pt</sub> )	% Weight ratio (Pt:Co:Cr)
Pt/C (Fuel Cell)	0.394	14.30	20:0:0
PtCoCrVu2Mi	0.278	16.17	3.5:0:1
PtCoCrV2Mi	0.218	19.09	5.6:0:2.2
PtCoCrVu2Na	0.298	20.52	5.3:1.7:0.8
PtCoCrV2Na	0.304	28.83	6.6:3.3:2.1

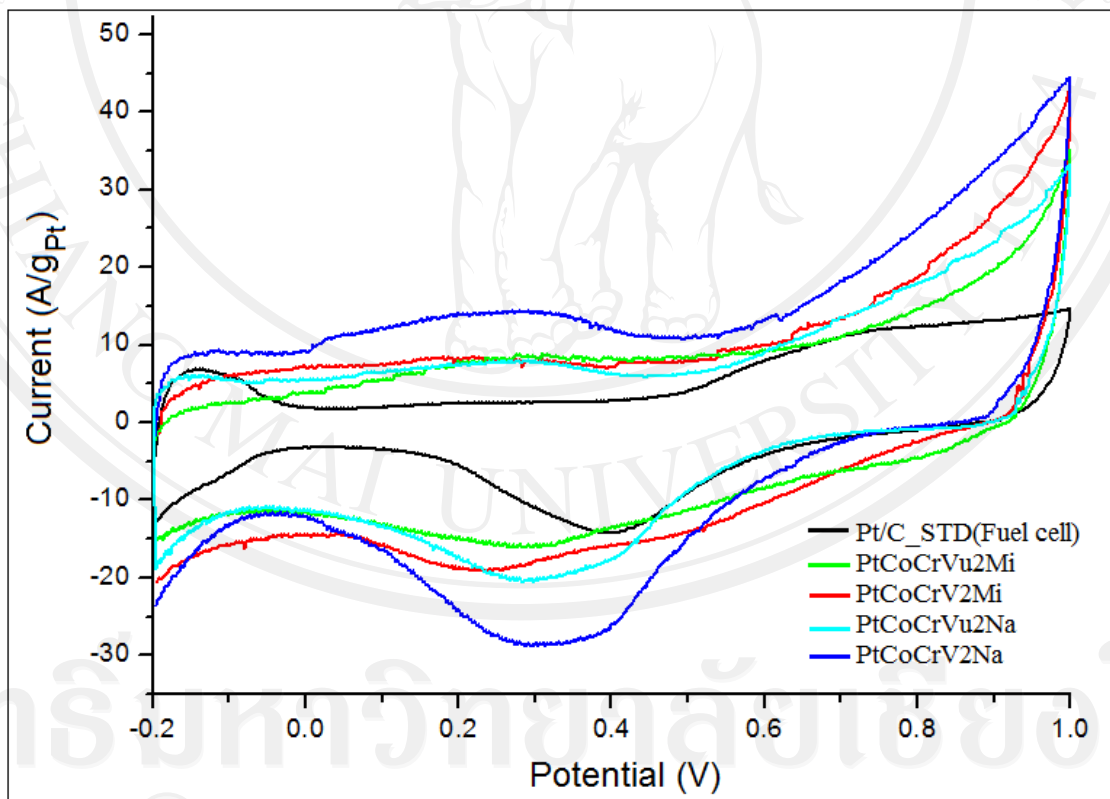
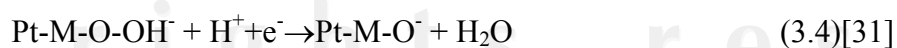
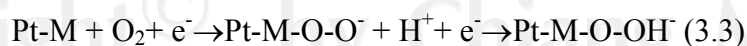


Figure 3.28 Cyclic voltammety spectra the first group catalyst and commercial 20 % Pt/C catalyst standard from Fuel Cells Scientific.

### 3.2.6 The single cell testing

Single cell testing was applied to study the sample PtCoCuN2Re, PtCuNiN2Na, PtCuNiN2Re, PtCuNiN6Na, PtCuNiN6Re, PtCuNiV2Na, PtCuNiV2Re, PtCuNiV6Na, and PtCuNiN6Re. These samples were confirmed by XRD and SAD patterns that the platinum alloy ternary catalysts on supported carbon was obtained. The results of PtCoCuN2Re and standard commercial catalysts tested by single cell testing were shown in Figure 3.29. The polarization curve was plotted between current density and voltage. The polarization curve of standard commercial Pt/C was similar to the curve from PtCoCu/C. At voltage of 600 mV, current density of the standard commercial and PtCoCu/C were 0.14 A/cm<sup>2</sup> and 0.18 A/cm<sup>2</sup>, respectively. However, the result from this graph was incomplete because the platinum weight between standard catalysts and prepared catalysts were not equivalent. By calculating platinum weight in catalysts per mole by using platinum weight from standard commercial as 20 %wt. and platinum weight from sample by EDS technique. The new polarization curve was shown in Figure 3.30. This graph showed the current density of that at 600 mV the standard commercial and PtCoCu/C as 14.81 and 22.57 kA/cm<sup>2</sup>.mol<sub>pt</sub>, respectively. It was found that PtCoCu on treated carbon N115 performed higher performance than standard catalysts without hydrogen-peroxide generation (Eq 3.3, 3.4). Moreover, it has high kinetic parameters such as Tafel slope and exchanged current density values [46].



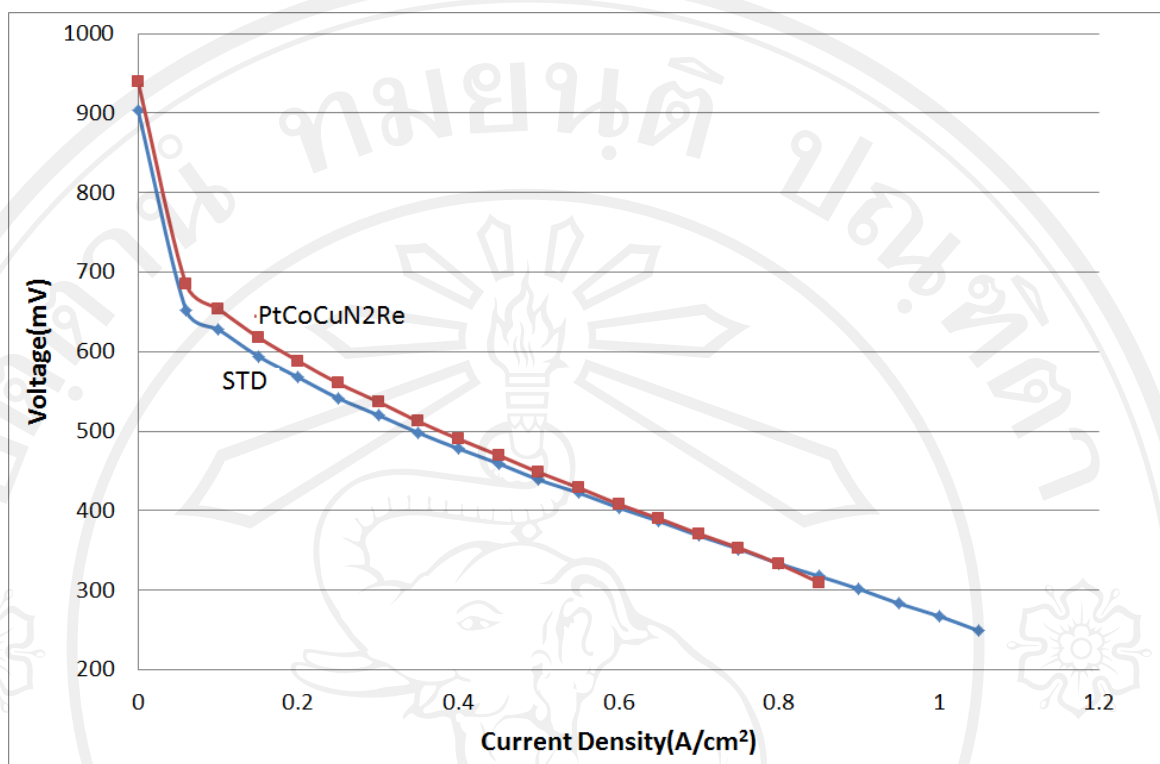


Figure 3.29 Polarization curves of standard commercial Pt/C and platinum-cobalt-copper catalysts supported on treated carbon by reflux method.

Figure 3.31 shows polarization curve from single cell testing of standard commercial catalyst comparing with and PtCuNiN2Na, PtCuNiN2Re, PtCuNiN6Na, PtCuNiN6Re, PtCuNiV2Na, PtCuNiV2Re, PtCuNiV6Na, and PtCuNiN6Re catalysts. The current density at 600 mV, particle sizes and weight ratio (from EDS) for catalysts was shown in Table 3.8. It was found that the catalysts prepared by  $\text{NaBH}_4$  reduction method shown higher performance than catalysts prepared by reflux method and standard commercial catalysts. The higher performance of catalysts prepared by  $\text{NaBH}_4$  reduction method was influenced by the smaller particle size than other catalysts (confirm by TEM). The fine particle catalysts performed better performance because active size was greater than large particle size catalysts [92]. The catalysts

prepared by  $\text{NaBH}_4$  reduction method used  $\text{NaBH}_4$  as a reducing agent. According to the reduction process of metal ion in Eq 1.9, if particle size of reducing agent was large, it would give more electrons to metal to grow [62]. The smaller size  $\text{NaBH}_4$  which dissolved in ethylene glycol, can reduce metal ion to metal and later form small size product. For reflux method which used ethylene glycol as a reducing agent, it had more electrons to donate to metal ion.

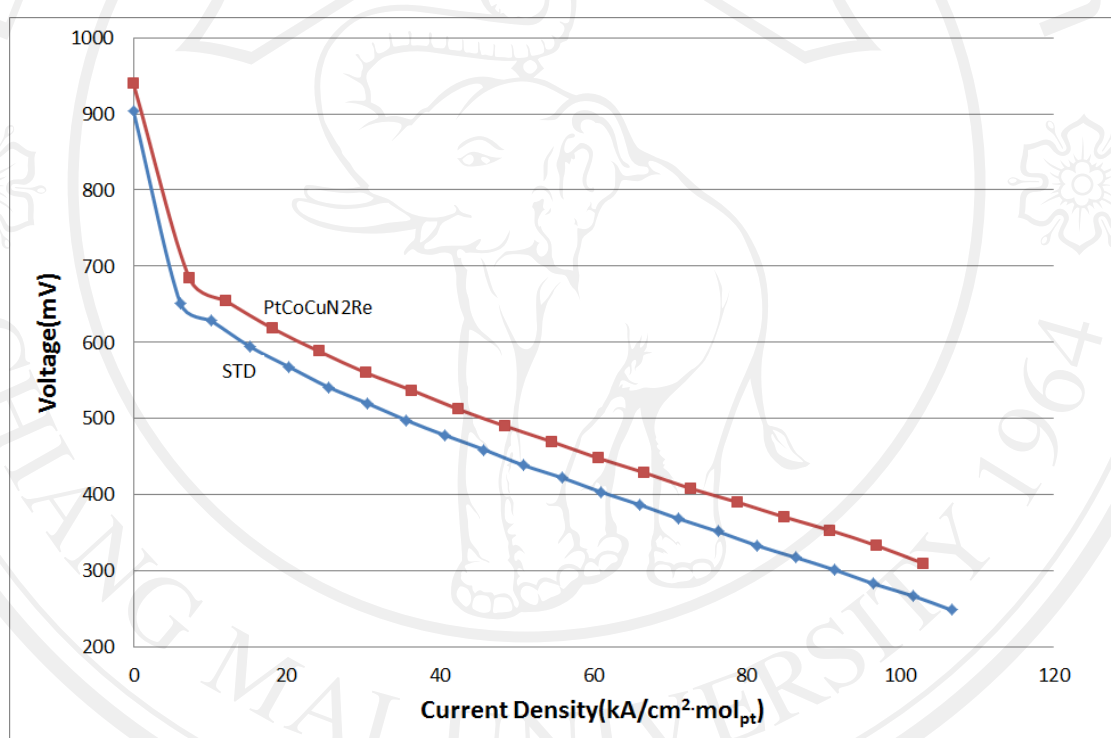


Figure 3.30 Polarization curves of standard commercial Pt/C and platinum-cobalt-copper catalysts supported on treated carbon by reflux method calculated per mole platinum.

Table 3.8 Current density of catalysts at 600 mV

Sample	Current density <sup>2</sup> (kA/cm <sup>2</sup> .mol <sub>pt</sub> )	Particle size (nm)	Weight ratio (Pt:M1:M2)
Pt/C STD	14.81	-	-
PtCoCuN2Re	22.57	4.09±0.69	10.28 : 0.17 : 5.30
PtCuNiN2Re	18.15	3.16±0.55	8.40 : 4.81 : 2.92
PtCuNiN6Re	14.81	3.46±0.88	12.34 : 2.45 : 2.56
PtCuNiV2Re	18.51	3.51±0.58	12.79 : 3.71 : 0.42
PtCuNiV6Re	24.44	3.96±0.67	10.32 : 2.18 : 0.29
PtCuNiN2Na	34.81	2.81±0.52	5.32 : 4.46 : 2.16
PtCuNiN6Na	42.96	2.75±0.56	10.17 : 1.55 : 0.27
PtCuNiV2Na	38.14	2.78±0.70	7.39 : 5.05 : 0.56
PtCuNiV6Na	54.07	2.73±0.55	9.37 : 2.72 : 1.02

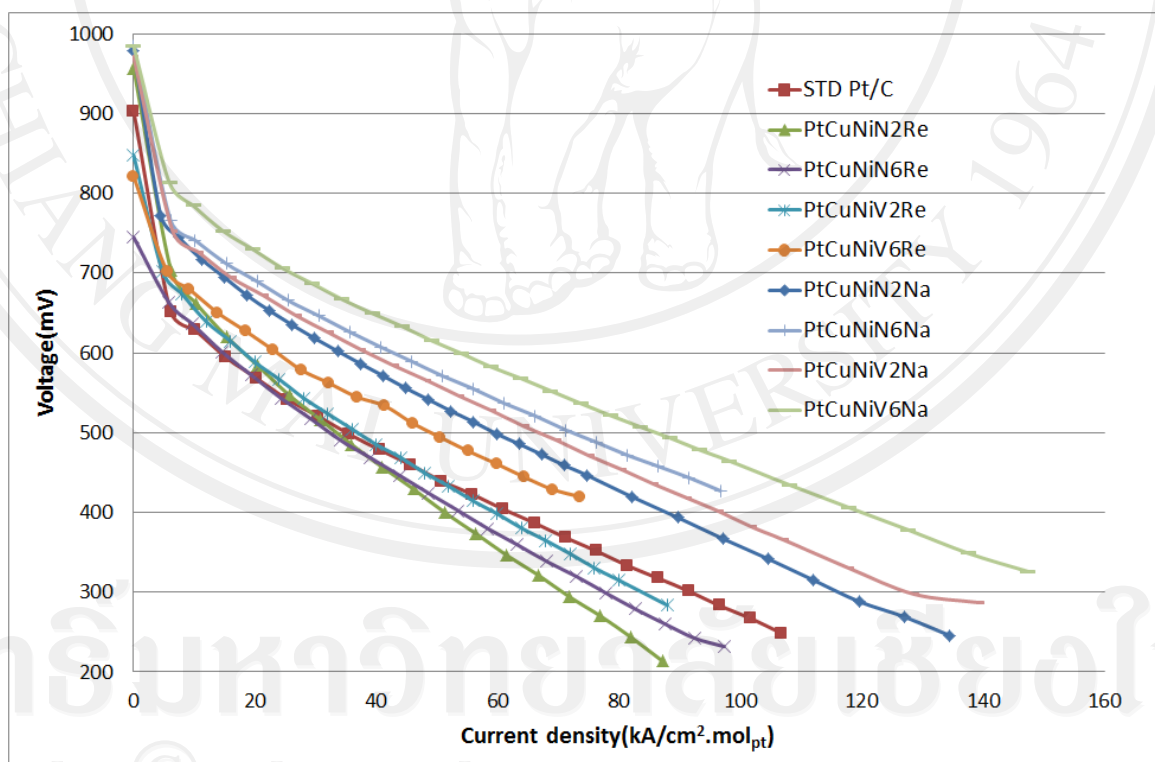
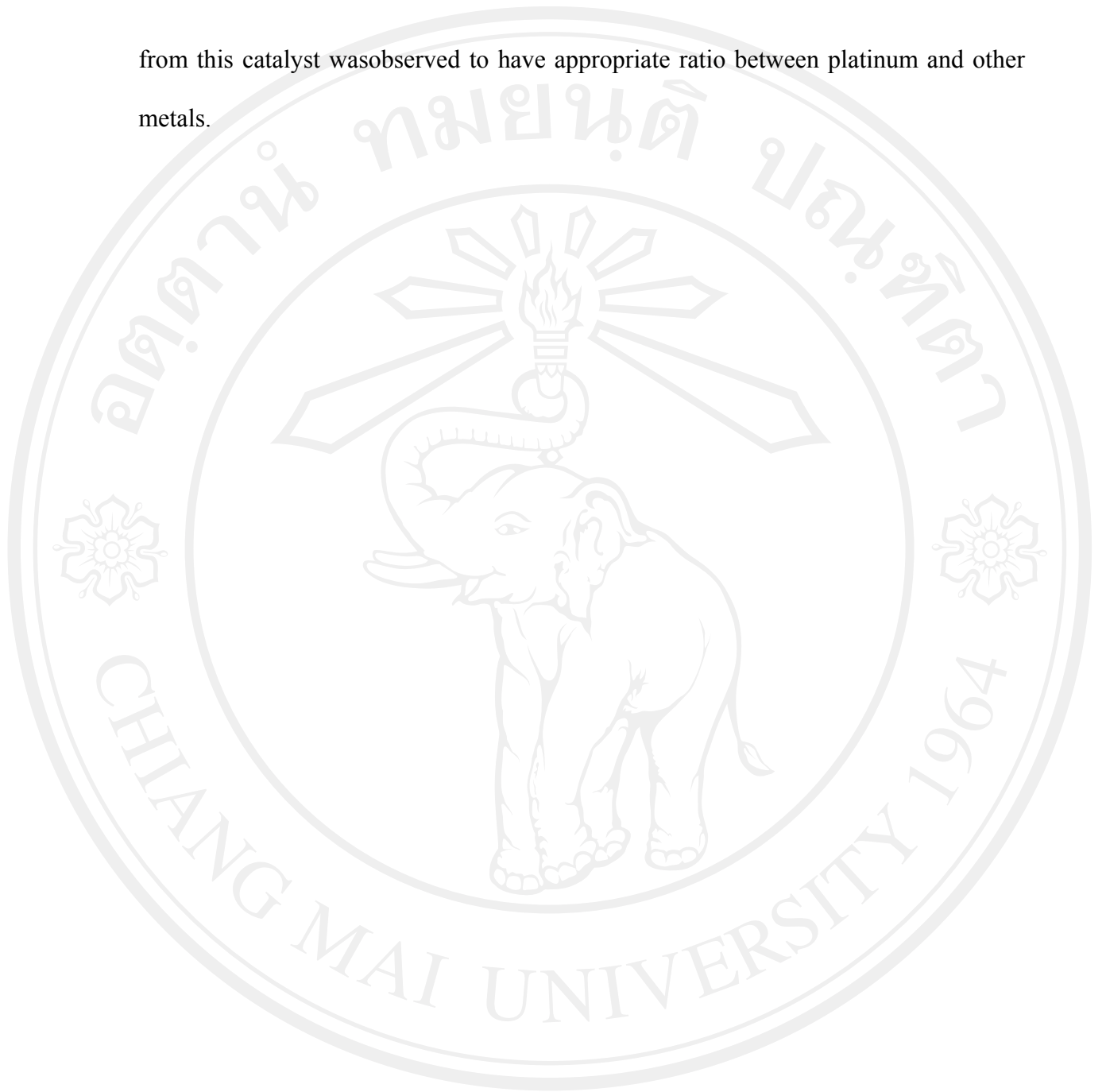


Figure 3.31 Polarization curves of standard commercial Pt/C and platinum-copper-nickel catalysts supported on treated carbons calculated per mole platinum.

Considering on the platinum-copper-nickel catalysts on carbon with different composition as 6:1:1 and 2:1:1, the ratio of 6:1:1 showed higher performance because the larger amount of transition metal was considered as important factor for determining the catalyst performance. The alloy with larger transition metal has increases the catalytic activities. However, the excess of transition metal can feasibly decrease the catalytic activities [46]. In summary, the platinum-copper-nickel with the ratio of 9:3:1 from EDS on carbon Vulcan XC-72 performed the highest performance among other catalysts in this part.

This research focused on the synthesis of platinum-based ternary catalysts for PEMFC cathode. The samples which were PtCoCuN2Re, PtCuNiN2Na, PtCuNiN2Re, PtCuNiN6Na, PtCuNiN6Re, PtCuNiV2Na, PtCuNiV2Re, PtCuNiV6Na, and PtCuNiN6Re, were confirmed by XRD and SAD patterns as metal alloy. The samples such as PtCoCrVu2Mi and PtCoCrV2Mi were confirmed phases as Pt-Cr<sub>2</sub>O<sub>3</sub> and PtCoCrVu2Na and PtCoCrV2Na were confirmed phases as Pt-CoO-Cr<sub>2</sub>O<sub>3</sub> by XAS technique. These samples were not tested by single cell test station because it was not formed as metal alloy. The metals (such as Pt, Co, Cr, Cu, Fe, and Ni) were found in all samples with EDS technique. The TEM images indicated that the catalysts were well dispersed on treated carbon. The particle size of catalysts prepared by NaBH<sub>4</sub> reduction method was smaller than those prepared by reflux method. Comparing the catalysts from this research, it can be concluded that the PtCuNiV6Na catalysts with the ratio of 9:3:1 showed the highest performance at the current of 54.07 kA/cm<sup>2</sup>.mol<sub>Pt</sub> and the voltage of 600 mV. The reason is because of this catalyst was confirmed by XRD as the platinum-based ternary alloy compound. The composition

from this catalyst was observed to have appropriate ratio between platinum and other metals.



ลิขสิทธิ์มหาวิทยาลัยเชียงใหม่  
Copyright© by Chiang Mai University  
All rights reserved